CHAPTER 5

Heavy metal removal using foam separation

Foam separation method was used to remove heavy metal solutes such as zinc, cadmium and nickel ions as well as their mixtures from aqueous solutions using sodium dodecyl sulfate as the foaming agent and collector. Solutes to be removed from the feed are adsorbed on the bubble surface and concentrated in the foam. Collected solutes are recovered in liquid foamate phase by disintegrating the foam. This chapter accounts for the metal recovery in the foamate, identification of the outlet for optimal recovery, effect of gas flow rate, pH, interaction of metal ions with a polymer on metal recovery. Mechanism of metal recovery process is identified using species distribution diagram. For the case of metal recovery as precipitated solids the particles formed were appropriately characterized. Floatation rate constants are evaluated and the separation is scaled to larger column size.

5.1 Factors influencing foam separations

Foam separation involves either the adsorption of ions or molecules on the surfactant producing the foam and moving out of the system with the foam formed or the capture of hydrophobic particles by air bubbles, which is accomplished in three distinct processes: collision, adhesion, and detachment, as shown in Fig. 5.1.

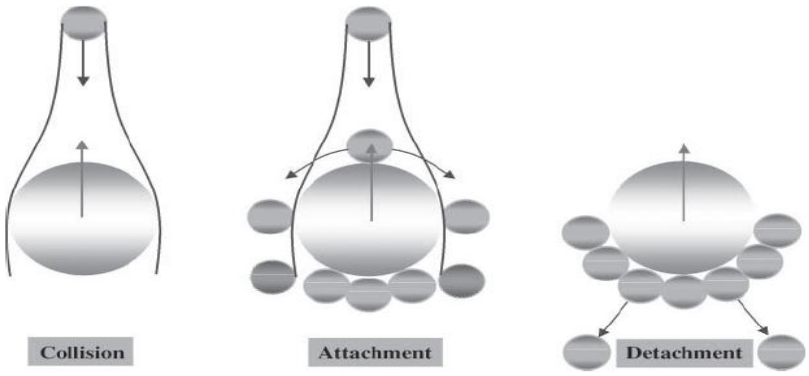

Fig. 5.1: Processes in Foam separation (Tao 2004)

Very often in metal removal by ion floatation or precipitate floatation both adsorption and attachment processes occur simultaneously. The low recovery of metal is mainly due to the low probability of bubble–particle collision, while the

main reason for poor recovery of coarse particles is the high probability of detachment of particles from the bubble surface. Use of smaller bubbles is the most effective approach to increase the probability of collision and reduce the probability of detachment.

The attachment process is selective and the difference in attachment probability of different particles determines the selectivity of flotation. The attachment process is determined by hydrodynamic and surface forces of particles and bubbles. The prediction of particle–bubble interaction in a real system depends on the gas holdup effect, the interaction between neighboring bubbles, and the presence of multilayers of bubbles, all of which tend to straighten the liquid streamlines around a bubble and thus increase the overall probability of collection.

The behavior of the foam phase is another important aspect of foam separation that affects performance. Separation efficiency can be improved if foam stability is properly controlled. In pure water bubbles coalesce with formation of one irregular large bubble. The rate of coalescence of these bubbles is fast. While in the presence of a small amount of surfactant no coalescence occurs and the bubbles are uniform in size and free of distortion.

At low gas flow rate higher retention times are needed. On the other hand high gas flow rates result usually in the formation of large amounts of wet foam, indicating a volume of entrained water, which is difficult to be handled. The bubble size and gas flow rate have been found to influence significantly the rate of removal.

5.2 Optimization of operational parameters.

Experiments were planned to study removal of heavy metals from aqueous solutions. Initial runs were designed to optimize process parameters. Feed solution containing 100 ppm zinc with metal to surfactant ratio (Zn: SDS) 1:2 on mole basis was charged in a glass column. The liquid loading in the column was fixed at 450 ml. In general it was observed that the foam emerging from O-1 outlet which was 47 cm above the liquid surface was very wet hence this outlet was not used to collect foam during removal of metal. The foamate was withdrawn from the outlet O-2 which was 92.5 cm above the liquid surface and a relatively dry foam was obtained from this outlet.

Blank runs, without metal content in feed but having similar amount of SDS solutions were also performed to gage the effect of presence of metal on foamate volume. Initial runs were performed for zinc removal that was evaluated at flowrates ranging between 0.02-0.08 lpm for time period ranging from 5-30 min. At the minimum flow rate of 0.02 lpm the foam does not climb up to the column outlet O-2 before 13-15 minutes, the flow rate was not enough to sustain continuous flow of foam from the outlet before this time. At low gas flow rate the foam drainage is rapid and quite dry foam having large bubbles appear at the upper edge of the foam.

However, once the flow of foam gets established even at 0.02 lpm gas rate, foam emerges out from the column uninterrupted. It is seen from Fig 5.2 that the foamate collected after 15minutes till 30 minutes at gas flow rates of 0.02 lpm shows increasing recovery of zinc in the foamate. At gas flow rates of 0.04 lpm and 0.06 lpm the recovery patterns of zinc from the feed at different times are more consistent, While at gas rates of 0.08 lpm the foam obtained from O-2 was quite wet and large recoveries of zinc was noted up to 15 minutes of foaming time thereafter the increment in recovery was not very significant.

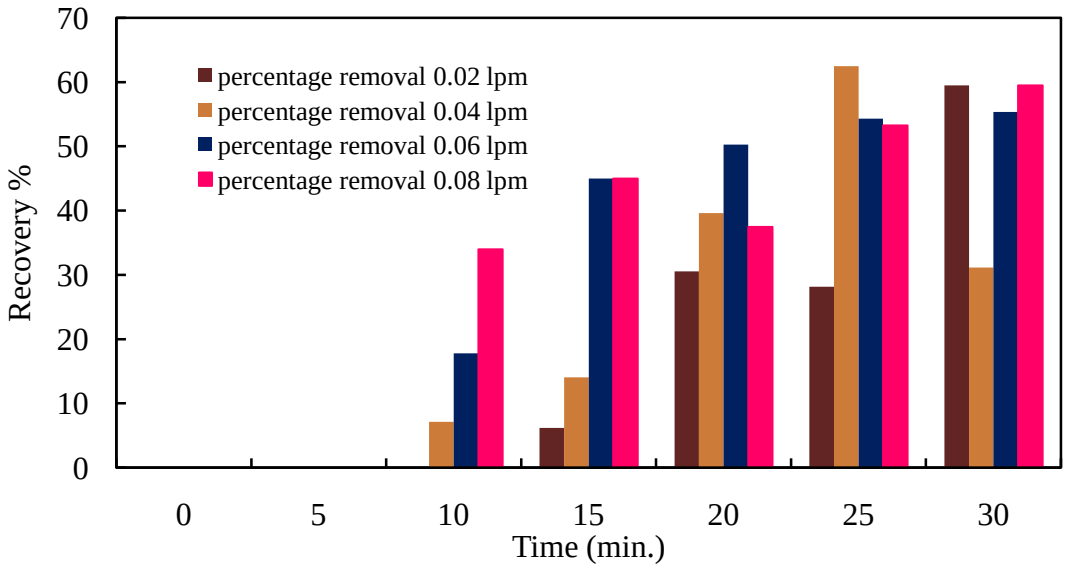

Fig.5.2: Percentage zinc removal at various flowrates and various time

It can be observed for the Fig. 5.2 that at all gas flow rates with the exception of gas flow rate of 0.06 lpm the recovery tends to dip arbitrarily at some run time between 10 to 30 minutes. This behavior is attributed to the complex

hydrodynamics of foam and its interaction with the device. Gas flow rate has significant effect on the resultant bubble size distributions. As the gas flow rate increases the number of bubbles with larger sizes also increases. The increase of gas flow rate yields more bubbles from the sparger and, thus, their population in the column. Consequently, the frequency of collisions between bubbles increases and bubble coalescence becomes more pronounced leading to relatively larger bubble sizes inside the column, these aspects affect the drainage pattern in the foam bed and the internal reflux in the column. For the foam column under consideration the gas flow rate of 0.06 lpm delivered the most consistent foam bed performance that is also reflected in the consistently increasing zinc recovery patterns at increasing time spans. In all subsequent experimental runs the gas flow rate was maintained at 0.06 lpm.

Foamate surfactant concentrations from outlet O-2 was also determined at time intervals ranging from 5 to 30 minutes at air flowrates ranging between 0.02 to 0.08 lpm and is shown in Fig. 5. 3.

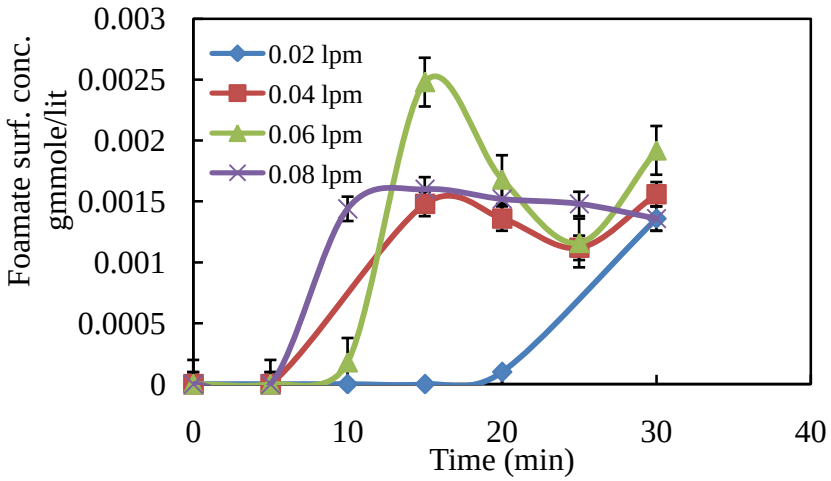

Fig. 5.3: SDS concentration in foamate at various flowrates

The pattern of foamate surfactant concentration observed at 0.02 lpm justifies that metal adsorbed on the surfactant is carried in foamate since increasing metal removal coincides with increasing surfactant concentration in foam. Foaming for 30 minutes results in foamate surfactant concentrations differing by 25% when air flow rates change from 0.02 lpm to 0.08 lpm, comparatively at 20 minutes foaming time the foamate surfactant concentrations at flow rates of 0.04 to 0.08 lpm varies

less than 10% as a result foaming time of 20 minutes per run was selected for all forthcoming runs.

The rising foam entrance with it substantial amount of solution that tends to reduce the concentration of the metal separated in the foamate, if a tall column of foam is provided most of the free liquid tends to drain down and only the liquid that forms the structural componetnt of foam that is present in liquid films and plateau borders would be present in the foamate. Since this amount of liquid is relatively very small the concentration of metal in the foamate that is transported by binding with the surfactant would be reasonably high. In the preliminary runs attempts were made to identify the location of the column outlet that would result in harnessing substantially dry foam.

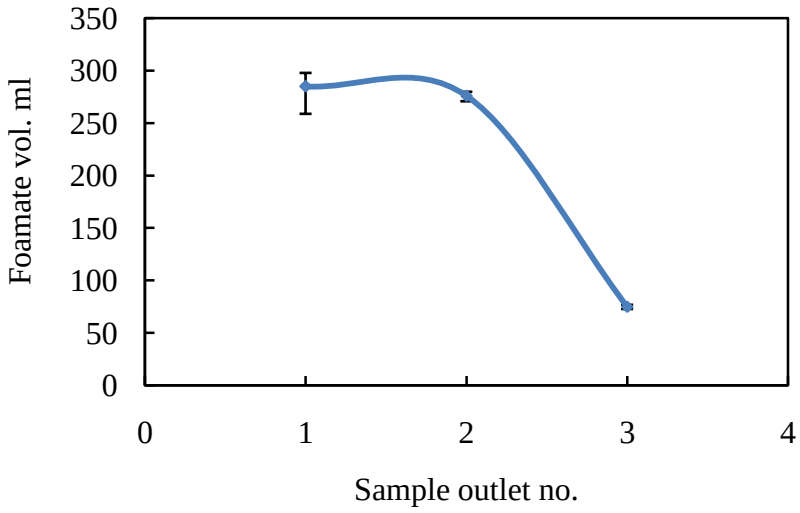

Fig. 5.4: Foamate volume collected for various sample outlets

For this purpose 450 ml of feed was charged in the column containing 100 ppm Zn and 0.0030 gmmole/lit SDS corresponding to Zn:SDS molar ratio of 1:2 and was foamed for 20 minutes duration at air flow rate of 0.06 lpm, the foamate was collected from sample ports O-1 which was 47 cm above the initial liquid surface, O-2 that was 92.5 cm above the initial liquid surface and O-3 located 157.5 cm above the initial liquid surface. Fig. 5.4 depicts the foamate volume collected in the three cases and it is clearly evident that outlet O-3 resulted in dry foam in comparison to the other outlets. Hence, in subsequent experiments the foamate was always collected from outlet O-3.

5.3 Mechanism of flotation of metal ions by SDS

Cationic heavy metals e.g. Cd^{2+}, $Zn^{2+}$and Ni^{2+} get removed from aqueous solution using an anionic surfactant due to their interaction with anionic functional groups on the surface of the surfactant. Exterior molecules with hydrophobic groups can be strongly bound by the van der Waals interaction and then can influence the characteristics of the surfactant's surface.

In an aqueous foamy dispersion containing anionic surfactants the hydrophilic head groups of the surfactant are oriented toward the aqueous phase, as a result the positive metal ions adsorb on to the surfactant. It is for this reason that the capacity of SDS to adsorb the metal is large. The interaction between metal and surfactant can be expressed by equation 5.1

$$2RSO_3Na + Me^{2+} \leftrightarrow (RSO_3)_2Me + 2Na^+ \qquad 5.1$$

Where Me is bivalent metal ion. Eq. 5.1 indicates that metal ions can easily approach and bind to the negatively charged groups of the anionic surfactant. Another possible reaction is a competitive or inhibition mechanism between surfactant and H^+ ion as shown in Fig 5.2

$$RSO_3Na + H^+ \leftrightarrow RSO_3H + Na^+ \qquad 5.2$$

It is reported that usually large amounts of metal ions are removed in polynuclear form by small amount of a surfactant.

Precipitate flotation is a process that involves concentration of the ionic species by forming initially some kind of precipitate and removal of the precipitate from the dilute aqueous dispersion by the transfer to surface by gas bubbles. In many ways it is an extension of conventional treatment processes of industrial aqueous streams for heavy metal removal where the metal ion is precipitated as hydroxide and then removed by settling of the precipitate. Precipitate flotation offers the advantage of lower surfactant requirement over ion flotation.

5.4 Zinc removal by foaming

5.4.1 Selection of sampling port

For a charge of 450 ml of feed solution the sample ports O-2 and O-3 of the foam column FC-1 located 92.5 cm and 157.5 cm above liquid level respectively were in contention. Under identical operating conditions of feed containing 100 ppm zinc having Zn:SDS 1:2 molar ratio, air flowrate of 0.06 lpm and 20 minute operation duration the recovery of zinc was 50% from port O-2 while from port O-3 it increased to 72% . Foamate volume collected was 276 ml from port O-2 while it was only 75 ml from port O-3. In view of the increased extent of metal removal and decrease in foamate volume it was decided to collect samples from port O-3.

5.4.2 Effect of pH

The most influential parameter in the foam separation of metal ions such as zinc, cadmium, copper etc. is pH because it determines the magnitude and sign of the charge on ions. Depending on the pH value of solution, the foam separation process may follow a different route i.e. through either ion or precipitate flotation. Knowing the type of species present in the solution helps to decide the appropriate surfactant, anionic or cationic, to use.

It is possible to know *apriori* with some confidence the nature of ionic species likely to be encountered at different pH conditions. The software Visual Minteq 2.15 was utilized to generate ionic species distribution diagrams at different zinc concentrations. (Ahn 2009). The ionic chemistry of zinc in aqueous solutions is shown in equation 5.3. $Zn(OH)^{+}$ is formed at the expense of Zn^{2+} ions at low pH values, poly nuclear zinc complexes such as $Zn_2(OH)^{3+}$ can also form.

$$Zn^{2+} + H_2O \Leftrightarrow Zn(OH)^{+} + H^{+} \quad 5.3(a)$$

$$Zn^{2+} + 2H_2O \Leftrightarrow Zn(OH)_2 + 2H^{+} \quad 5.3(b)$$

$$Zn^{2+} + 3H_2O \Leftrightarrow Zn(OH)_3^{-} + 3H^{+} \quad 5.3(c)$$

$$Zn^{2+} + 4H_2O \Leftrightarrow Zn(OH)_4^{2-} + 4H^{+} \quad 5.3(d)$$

$$Zn(OH)_2(s) \Leftrightarrow Zn(OH)_2(aq) \quad 5.3(e)$$

Fig 5.5 (a), (b) and (c) show the specie distributions at initial concentrations of 50, 100 and 200 ppm as a function of pH.

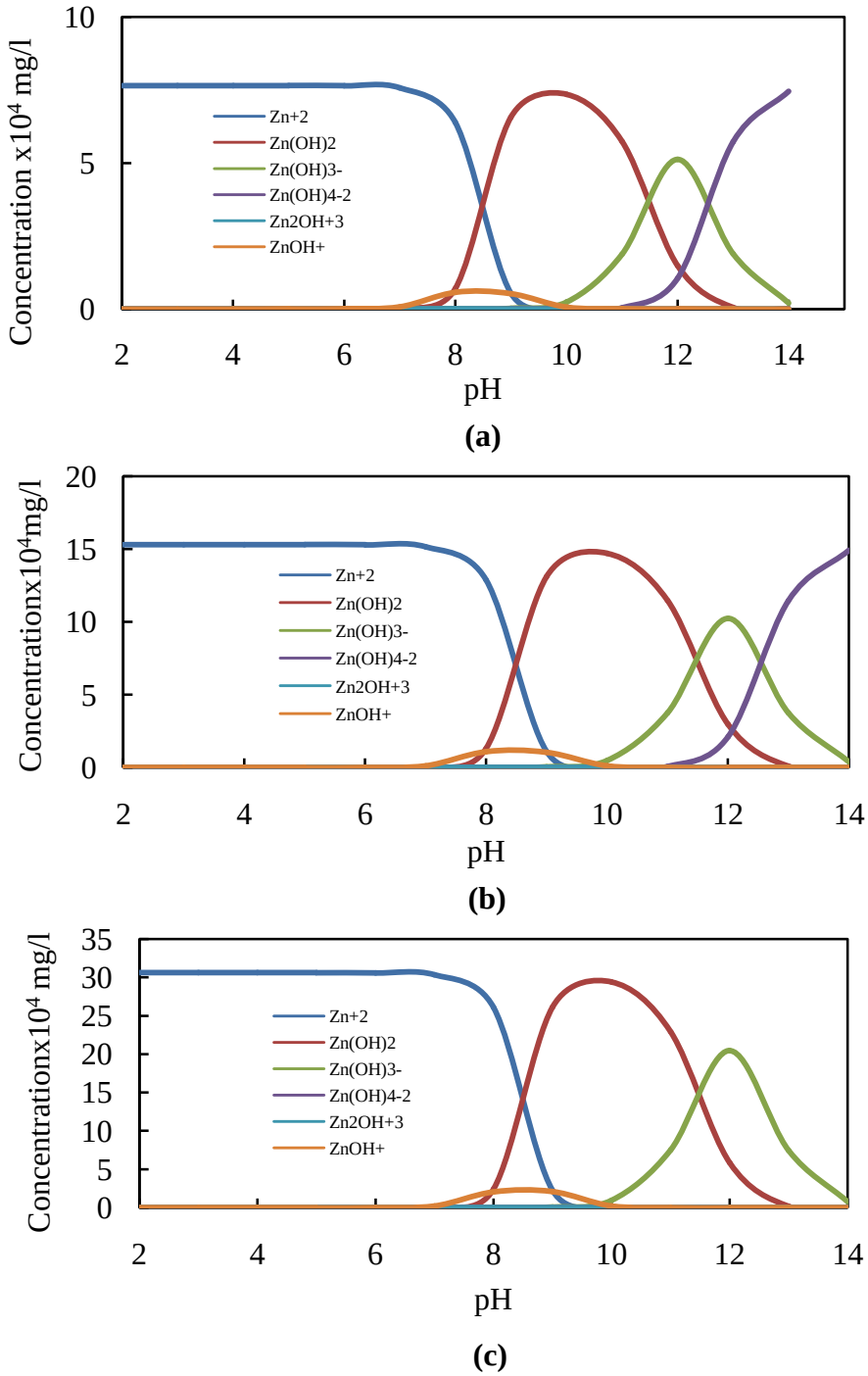

Fig. 5.5: Species distribution for (a) 50 ppm (b) 100 ppm (c) 200 ppm zinc in water

It is seen from Fig. 5.5 (a) that there are negatively and positively charged zinc species between pH 2 and 14. For pH values between 2 and 7, zinc and its species are positively charged, however, for pH values higher than 7 they are

negatively charged. For zinc, the speciation was calculated as a function of pH, based on equations 5.3(a) to 5.3(e).

The speciation diagram for 100 and 200 ppm zinc sulfate is shown in Fig.5.5(b) and 5.5 (c) respectively. At 100 ppm zinc concentrations, the zinc ion, Zn^{2+}, is the dominant specie up to pH 9 while zinc hydroxide, $Zn(OH)_2$ is the dominant species from pH 9 to pH 11. Above pH 10, $Zn(OH)_3^-$ formation occurs according to Equation 5.3(c) and above pH 11, $Zn(OH)_4^{2-}$ formation takes place according to Equation 5.3(d).

The effect of pH on zinc recovery was investigated in the pH range of 4 to 11 in this range polynuclear zinc species are unlikely to be formed. The initial feed concentration for all these runs was C_{Fi} = 100 ppm zinc, other parameters were Zn :SDS molar ratio = 1:2, Initial feed charged = 450 ml, air flow rate = 0.06 lpm, duration of foaming = 20 minutes. Foam was collected from sample port O-3 in the whole duration of the run, foamate volume collected was measured and the foamate was analyzed for metal content.

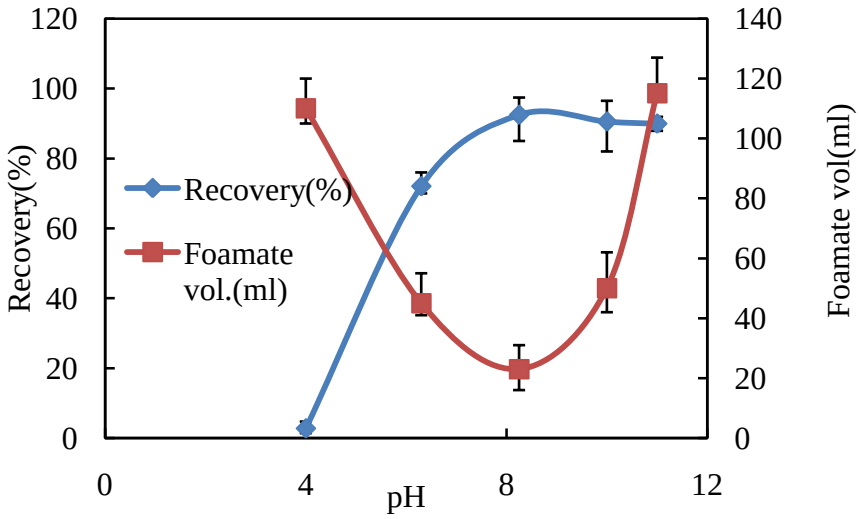

Fig. 5.6: Effect of pH on zinc recovery and foamate volume (C_{Fi} = 100 ppm)

Fig. 5.6 gives the zinc recovery profile and foamate volume profile as a function of initial pH. It can be seen that the recovery begins at pH 4 and increases exponentially till pH 8 and then almost remains constant. Conditions ensuring ion floatation of Zn^{2+} ions almost ends by pH 9 and precipitate floatation begins and as a result the sensitivity of zinc recovery to pH ceases.

At lower pH values the lower extent of zinc recovery can be attributed to competition of hydrogen ions with the metal cations for the available surfactant sites. (Jurkiewicz 1990).

Foamate volume decreases from 110 ml to 23 ml as pH increases from 4-8. Foamate volume is 50ml for pH 10 and 115 ml for pH 11. The enrichment of the gas bubble-solution interface with sodium dodecyl sulfate also results in increased thickness of the water sheath around the bubble and consequently in increased foam hydration. Besides compression of the electric double layer, specific adsorption of the surfactant directly affects the increased hydration of gas bubbles. The surfactant SDS is capable of dissociating and exchanging Na^+ for other metal cation species thereby reducing its capacity to bind with Zn^{2+} during foam separation.

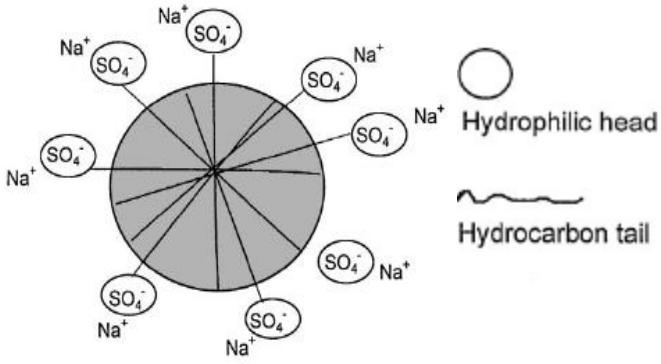

Fig. 5.7: Structure of SDS (Zhong 2000)

At high NaOH concentration for higher pH the charge of RSO_4^- anions in the adsorption layer of gas bubbles is more rapidly neutralized by Na^+. Closer packing of hydrated $RSO_4^-Na^+$ ion pairs takes place in the surface layer as shown in Fig 5.7. As a result the water sheaths of gas bubbles become more stable and thicker resulting higher foamate volume. Hence wet foam with less zinc concentration in foam was obtained. For maximum zinc removal foamate volume obtained is minimum. The increased recovery in such case is not due to hydraulic entrainment.

According to Karger et al. (1968), the product of reaction in Eq. 5.4 zinc dodecyl sulfate is identified as being in the form of a hydrated ionic pair ($2RSO_4^-Zn^{2+}$)(H_2O)n. The product of reaction is removed by gas bubbles.

$$Zn^{2+} + 2(RSO_3^-Na^+) \rightarrow (RSO_3^-)_2Zn^{2+} + 2Na^+ \quad 5.4$$

The gas-bubble solution interface is enriched with zinc dodecyl sulfate results in more recovery of metal zinc and less foamate volume.

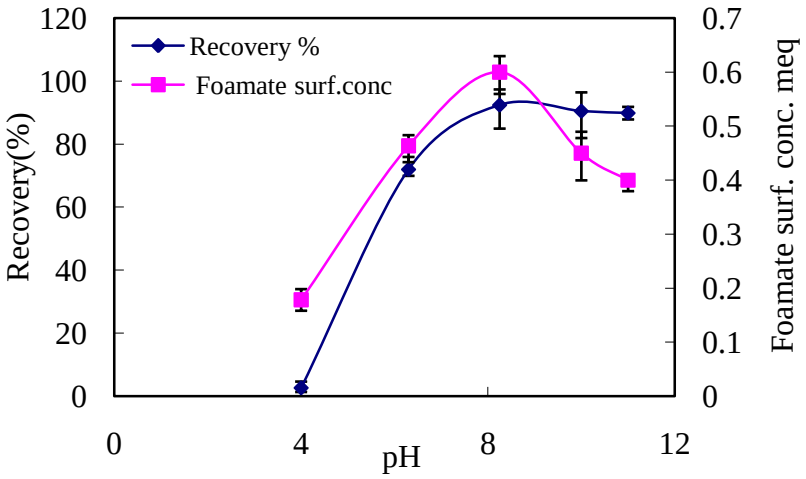

Fig. 5.8: Zinc removal and foamate surfactant concentration vs pH

Fig. 5.8 shows percentage zinc removal and foamate surfactant concentration as a function of pH. For higher zinc removal surfactant concentration in foamate is also higher indicating metal-surfactant complex formation and ion adsorption till pH 8. After pH 8 though foamate surfactant concentration is less metal removal is more indicating zinc hydroxide removal is by bubble association and not by ion adsorption.

5.4.3 Effect of SDS concentration

The effect of the SDS concentration on the removal of zinc was investigated at pH 8.25 for feed zinc concentrations of 100 ppm at an air flowrate 0.06 lpm and 20 minutes foaming time. Samples were collected from the O-3 sample port varying surfactant concentrations from 0.0015 to 0.0060 gmmole/lit corresponding to molar ratio of Zn to SDS of 1 to 4.

Fig. 5.9(a) shows percentage recovery and foamate volumes obtained for various metal: surfactant Zn:SDS mole ratios. Foamate volume decreases from 100 to 80 ml as surfactant concentration increases. This behavior could be attributed to decrease in bubble monodispersity since higher surfactant concentration increases

the coalescence rates. Zinc recoveries were 64%, 92%, 18% and 44% for Zn : SDS initial molar ratios of 1:1, 1:2, 1:3 and 1:4 respectively.

At pH of 8.25 the dominant mode of transport of metal is expected to be precipitate floatation as per Fig. 5.4 (b) under such conditions the decline in zinc removal with increasing SDS concentration was analyzed by Beheir et. al. (1996).

They opine that separation results when a condensed layer of the surfactant (a hemimicelle) is formed on the solid surface with the ionic heads on the solid and hydrocarbon tails pointing to the solution thus the solid surface becomes hydrophobic permitting gas bubble attachment and separation.

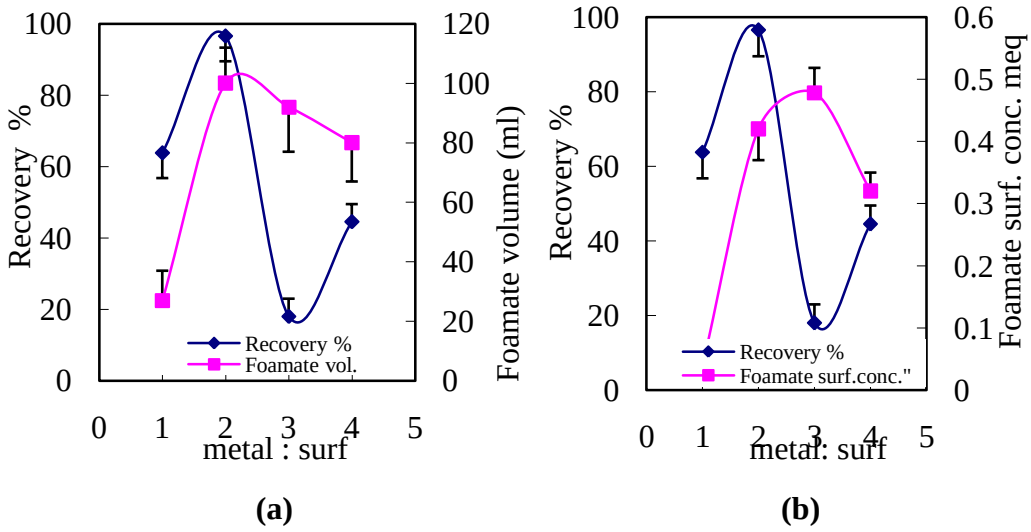

Fig.5.9: (a) Effect of Zn: SDS molar ratio on foamate volume & zinc removal (b) Effect of Zn:SDS on foamate surfactant concentraion & zinc removal (C_{Fi} = 100 ppm Zn, pH = 8.25)

At exceedingly high surfactant concentrations, a second hemimicelle is formed on top of the first one with the ionic heads pointing to the solution thus yielding a hydrophilic surface with the result that the precipitate fails to attach.

Fig. 5.9(b) shows percentage recovery and foamate surfactant concentration at various metal:surfactant molar ratios. The pattern of foamate surfactant concentration justifies that metal adsorbed on the surfactant is carried in foamate since increasing metal removal coincides with increasing surfactant concentration in foam.

5.4.4 Effect of Zinc concentration in the feed

The effect of the feed zinc concentration on the removal of zinc was also investigated at pH 8.25 at initial zinc concentrations of 50, 100 and 200 ppm while keeping the molar ratio of Zn : SDS = 2 in all cases all other operational parameters were kept identical. All samples were collected from O-3 sample port at air flowrate of 0.06 lpm.

Experiments were also performed with variation in the initial zinc concentration in the range of 50 ppm to 200 ppm but at constant surfactant concentration of 0.0030 gmol/lit which resulted in the variation of Zn to SDS molar ratio of 1:4 (for 50 ppm Zn concentration) to 1:1 (for 200 ppm Zn concentration) Table 5.1 shows Zn recovery at various Zn:SDS molar ratios for 50 and 200 ppm Zn.

Table 5.1: Zinc removal for various Zn:SDS molar ratios

Zinc conc. ppm	**Zn:SDS Molar ratio**	**Recovery %**
50	1:2	63.62
50	1:4	52.84
100	1:2	92.43
100	1:4	44.5
200	1:1	30.42
200	1:2	24.94

Zn removal of 63.62% was obtained for 50 ppm zinc with Zn:SDS 1:2 molar ratio. Removal decresed to 52.84% for Zn:SDS 1:4 molar ratio. This is attributed to competition between OH^- and dodecyl ions ions for Zn^{2+} separation. For 200 ppm zinc and Zn:SDS 1:1 molar ratio percentage removal was 30.42% and for Zn:SDS 1:2 molar ratios zinc recovery was 24.94%. Sodium dodecyl sulfate exhibited poor performance for 200 ppm zinc with Zn: SDS 1:1 and 1:2 molar ratio. An unstable foam formed on top of the solution, resulting in redispersion of the floated particles resulting in lesser metal recovery. Zn removal of 92.432% was obtained for 100 ppm zinc with Zn:SDS 1:2 molar ratio. Removal decresed to 44.5% for Zn:SDS 1:4 molar ratio.

From these results it became clear that foam separation worked better with low concentrations of zinc. While for higher zinc concentrations the removal efficiency is decreased. It becomes clear that in each system an optimum molar ratio of reagents could exist.

5.5 Cadmium removal by foaming

Cadmium recovery was also investigated on similar lines as zinc recovery in the same foam column and effect of pH and surfactant concentrations were investigated for fixed feed concentration of 100 ppm cadmium. 450 ml of feed solution was charged in the column and foam samples were withdrawn from sample port O-3 that was located 157.5 cm above the initial liquid level. Air flow rate was maintained at 0.06 lpm and the cadmium to surfactant Cd:SDS molar ratio was 1:2. Total operational time was 20 minutes.

5.5.1 Effect of pH on cadmium removal

The speciation nature of cadmium sulfate in water corresponding to 100 ppm of cadmium i.e the initial feed concentration in this investigation is shown in *Fig. 5.10* obtained using the Visual Minteq 2.15 software.

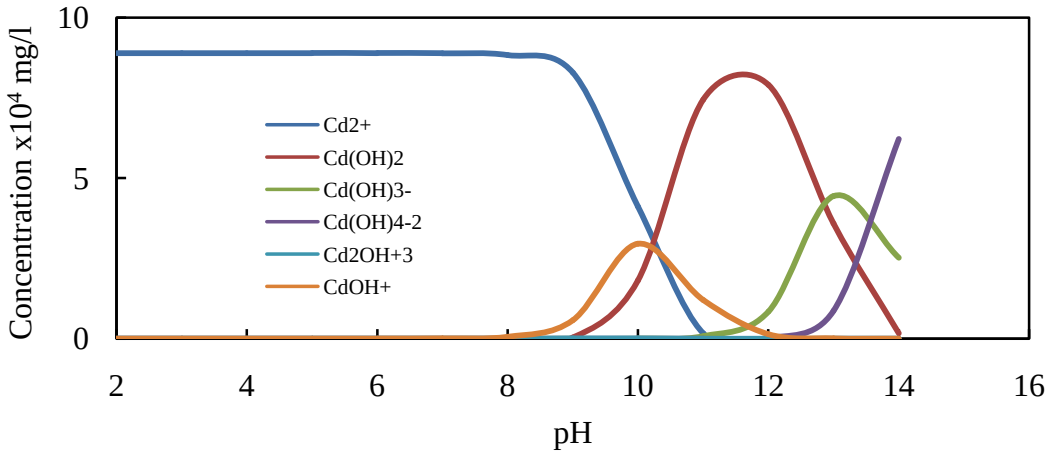

Fig. 5.10: Species distribution of 100 ppm cadmium in water

Cd^{2+} is the main ion present in solution for pH < 8. Above pH 9 in basic conditions most Cd is present as $Cd(OH)_2$. $Cd(OH)_3^-$ formation starts at pH 11 while at pH 12 or above, the main cadmium specie is $Cd(OH)_4^{2-}$. Polynuclear cadmium complex such as $Cd_2(OH)_3^+$ is also present.

The speciation was calculated as a function of pH, based on equations 5.5(a) to 5.5(e). The fraction of cadmium species such as Cd^{2+}, $Cd(OH)^{+}$, $Cd(OH)_2$, $Cd(OH)_3^{-}$ and $Cd(OH)_4^{2-}$ in solution varies over a range of pH .

$$Cd^{2+} + H_2O \Leftrightarrow Cd(OH)^{+} + H^{+} \quad 5.5(a)$$

$$Cd^{2+} + 2HO \Leftrightarrow Cd(OH)_2 + 2H^{+} \quad 5.5(b)$$

$$Cd^{2+} + 3H_2O \Leftrightarrow Cd(OH)_3^{-} + 3H^{+} \quad 5.5(c)$$

$$Cd^{2+} + 4H_2O \Leftrightarrow Cd(OH)_4^{2-} + 4H^{+} \quad 5.5(d)$$

$$Cd(OH)_2(s) \Leftrightarrow Cd(OH)_2(aq) \quad 5.5(e)$$

The effect of solution pH on cadmium removal along with accompanying foamate volumes is shown in Fig. 5.11(a).

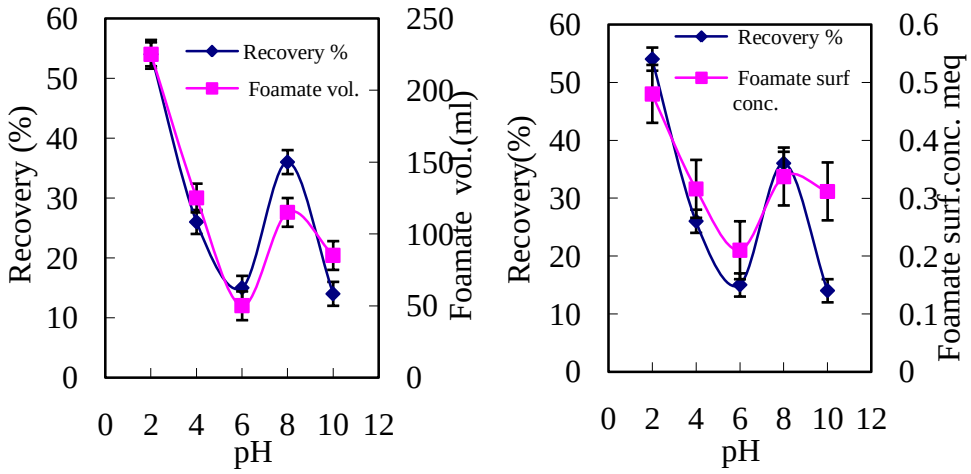

(a) **(b)**

Fig 5.11: (a) Effect of pH on cadmium recovery and foamate volume (b) Cadmium recovery and foamate surfactant concentration versus pH (C_{Fi} = 100 ppm, Cd:SDS molar ratio1:2)

Maximum cadmium recovery 54% was obtained at pH 2, which also corresponds to the maximum foamate volume observed. The profile of foamate volume and cadmium recovery follows the same pattern. This pattern of metal recovery is attributed to ion-adsorption, the adsorption of Cd^{2+} ions on SDS molecule leads to the transport of Cd-SDS complex with the ascending bubbles of the foam that tends to carry the Cd^{2+} ions from feed to foamate.

The foamate surfactant concentration also behaves identically except at high pH values wherein the metal recovery in the foamate is poor and out of tune with the foamate volume and surfactant concentration in the foamate as shown in Fig.

5.11(b). The pattern of foamate surfactant concentration justifies that metal adsorbed on the surfactant is carried in foamate since increasing metal removal coincides with increasing surfactant concentration in foam.

Cadmium recovery was just 15% at pH 6 and the foamate volume was ~ 50ml which shows a direct correlation between the Cd recovery in foam with volume of foamate transported. Even between pH 8 and 10, Cd^{2+} ion flotation is considered to be the cause of metal recovery. Significant concentration of hydrated precipitate of $Cd(OH)_2$ can be formed at pH > 9 which is confirmed by specie distribution diagram of cadmium sulfate.

The divalent cadmium cation (Cd^{2+}) is most abundant below pH 8. As pH is increased toward the precipitation point the concentration of metal polynuclear species also increases. Cadmium polynuclear species e.g., $CdOH^{+}$, $Cd(OH)_4^{-2}$ and $Cd(OH)_3^{-}$ do not bind well with SDS as does Cd^{+2} which has a higher charge density and more coordination sites available for surfactant SDS.

This behavior is apparent in Fig. 5.11(a) where a considerable decline in recovery of cadmium is observed at pH 10 although foamate surfactant concentrations were quite high.

5.5.2 Effect of SDS concentration

The effect of the SDS concentration on the removal of cadmium was investigated at pH 2 for feed cadmium concentrations of 100 ppm at an air flowrate 0.06 lpm and 20 minutes foaming time by varying the cadmium to SDS molar ratios. Samples were collected from O-3 sample port varying surfactant concentrations in the range of 0.00089 to 0.0035 gmmole/lit corresponding to variation of Cd:SDS mole ratios in feed from 1:1 to 1:4.

Fig. 5.12(a) shows percentage recovery and foamate volumes obtained for various Cd:SDS mole ratios. Foamate volume decreases from 225 ml to 160 ml as surfactant concentration increases from 0.00089 to 0.0035 gmmole/lit. This behavior is attributed to decrease in bubble mono dispersity, since higher surfactant concentration causes an increase in the coalescence rates. Cadmium

recoveries were 2%, 54%, 42% and 20% for Cd : SDS initial molar ratios of 1:1, 1:2, 1:3 and 1:4 respectively.

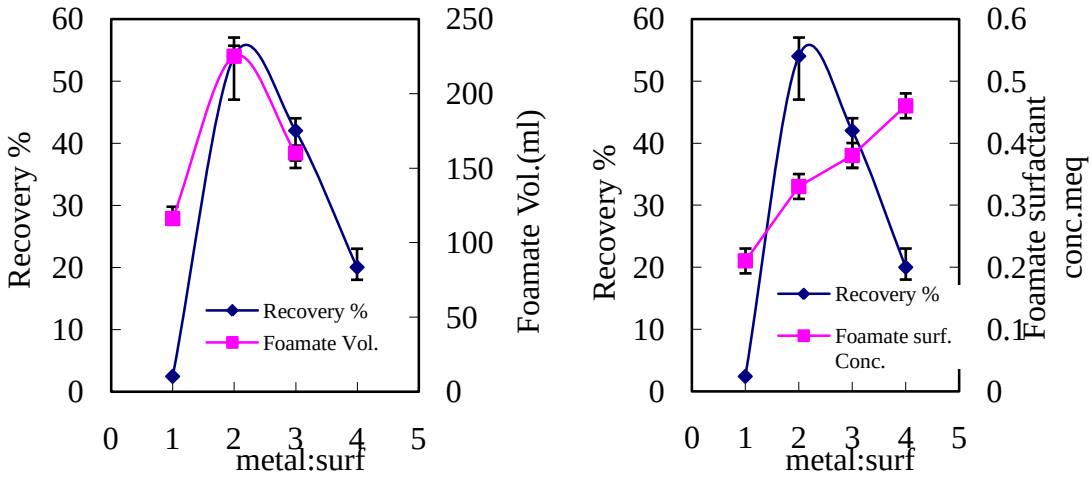

(a) **(b)**

Fig. 5.12: (a) Effect of Cd: SDS molar ratio on foamate volume and cadmium removal (b) Effect of Cd:SDS on foamate surfactant concentraion (C_{Fi} = 100 ppm Cd, pH = 2)

Fig. 5.12(b) shows percentage recovery and foamate surfactant concentration at various Cd:SDS molar ratio. The pattern of foamate surfactant concentration justifies that metal adsorbed on the surfactant is carried in foamate since increasing metal removal coincides with increasing surfactant concentration in foam. Decline in cadmium recovery at high surfactant concentrations is attributed to the same reasons that was discussed in Sec 5.4.3 for zinc removal, wherein masking of binding sites on the surface of a surfactant micelle occurs due to formation of hemimicelles.

5.6 Nickel removal by foaming

Nickel recovery was also investigated on similar lines as zinc and cadmium recovery in the same foam column and effect of pH on Ni recovery was investigated for initial feed concentration (C_{Fi}) of 100 ppm nickel. Feed solution (450 ml) containing Ni and SDS was charged in the column and foam samples were withdrawn for total operational time of 20 minutes from sample port O-3 that was located 157.5 cm above the initial liquid level. Air flow rate was maintained at 0.06 lpm and the nickel to surfactant Ni:SDS molar ratio was 1:2.

5.6.1 Effect of pH on nickel removal

The speciation nature of nickel sulfate in water corresponding to the initial feed concentration of 100 ppm of Ni is shown in *Fig. 5.13* that was obtained using the Visual Minteq 2.15 software.

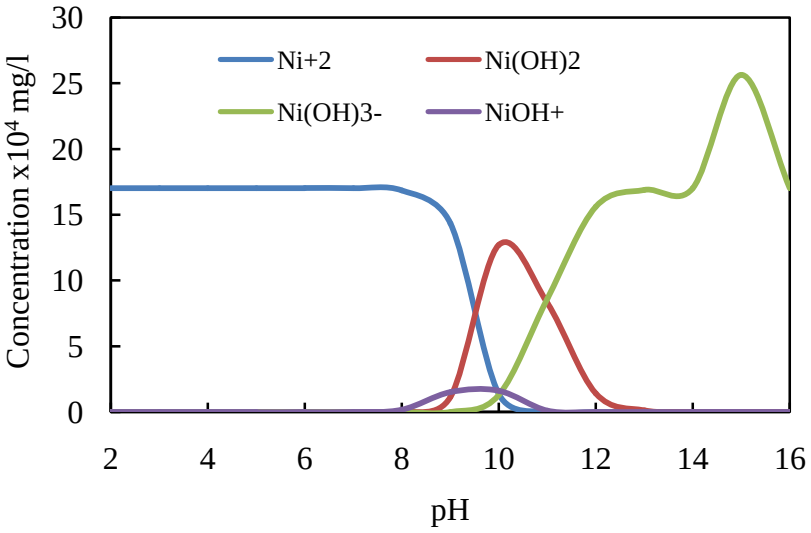

Fig. 5.13: Species distribution of 100 ppm Nickel in water

The chemical equations representing the ionic chemistry of nickel in aqueous media at different pH conditions are shown in Eq. 5.6(a) to 5.6(d). The fraction of nickel species such as Ni^{2+}, $Ni(OH)^{+}$, $Ni(OH)_2$ and $Ni(OH)_3^{-}$ in solution varies over a range of pH. Ni^{2+} is the main ion present in solution till pH 8. Above pH 9 in basic conditions most Ni is present as $Ni(OH)_2$. At pH 9, $Ni(OH)_3^{-}$ formation begins and at pH 12 or above, the main nickel specie is $Ni(OH)_3^{-}$.

$$Ni^{2+} + H_2O \Leftrightarrow Ni(OH)^{+} + H^{+} \quad 5.6(a)$$

$$Ni^{2+} + 2H_2O \Leftrightarrow Ni(OH)_2 + 2H^{+} \quad 5.6(b)$$

$$Ni^{2+} + 3H_2O \Leftrightarrow Ni(OH)_3^{-} + 3H^{+} \quad 5.6(c)$$

$$Ni(OH)_2(s) \Leftrightarrow Ni(OH)_2(aq) \quad 5.6(d)$$

The effect of solution pH on nickel removal along with accompanying foamate volume collected is shown in Fig. 5.14(a). Maximum nickel recovery was 31%, obtained at pH 8 which also corresponds to the higher foamate volume observed. The profile of foamate volume and nickel recovery follows the same pattern. This pattern of metal recovery is attributed to ion-adsorption, the adsorption of Ni^{2+}

ions on SDS molecule leads to the transport of Ni-SDS complex with the ascending bubbles of the foam that carries the Ni^{2+} ions from feed to foamate.

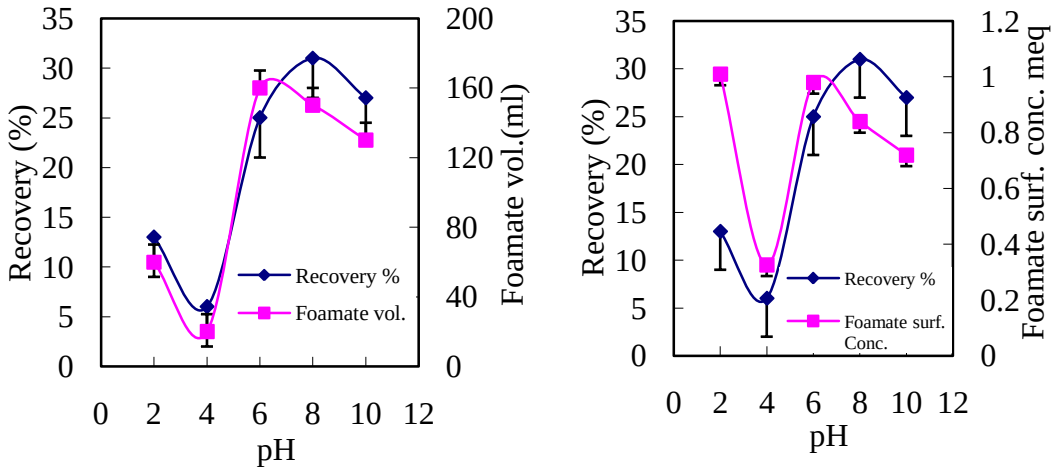

(a) (b)

Fig. 5.14: (a) Nickel recovery vs pH (b) Foamate surfactant concentration versus pH (C_{Fi} = 100 ppm Ni, Ni: SDS molar ratio 1:2)

The foamate surfactant concentration also behaves identically except at low pH values wherein the metal recovery in the foamate is poor and out of tune with the foamate volume and surfactant concentration in the foamate as shown in Fig. 5.14(b). The pattern of foamate surfactant concentration justifies that metal adsorbed on the surfactant is carried in foamate since increasing metal removal coincides with increasing surfactant concentration in foam.

The divalent nickel cation (Ni^{2+}) is most abundant below pH 8. As pH is increased toward the precipitation point the concentration of metal polynuclear species increases. Nickel polynuclear species e.g., $NiOH^{+}$, $Ni(OH)_3^{-}$ do not bind as well with SDS as Ni^{+2} which has a higher affinity for surfactant SDS. This behavior is apparent in Fig. 5.14 where a decline in recovery of Ni is observed at pH 10. Nickel recovery was just 13% at pH 2 and the foamate volume was ~ 60ml which shows a direct correlation between the Ni recovery in foam with volume of foamate transported. Even between pH 8 and 10, Ni^{2+} ion flotation is considered to be the cause of metal recovery. Significant concentration of hydrated precipitate of nickel $Ni(OH)_2$ is formed at pH > 9 which is confirmed by specie distribution diagram of nickel sulfate.

Effect of SDS concentration on nickel recovery was not investigated since it was expected that the behavior would not be any different from that of the two bivalent metals zinc and cadmium for which maximum removal was obtained at metal: surfactant molar ratio of 1:2.

5.7 Selective removal from Zinc-Cadmium and Nickel-Cadmium binary mixtures

The removal of metal ions from solutions of binary metal ion systems was investigated for the zinc-cadmium binary ionic system and the nickel-cadmium ionic system at varying pH with the objective to determine the selectivity of the separation. The selectivity of the separation process is mainly caused by the selective binding of metal ions to the surfactant ions. The surface inactive metal ions attach to the ionic surfactant of opposite charge. The actual mechanism of attachment of the surface inactive ion to the surfactant ion depends on the system.

The layer of anionic surfactant adsorbed at the air liquid system has associated with it a diffuse layer of ions of opposite charge in order to maintain electrical neutrality. The fact that counter ions associated with the anion layer would consist of a mixture of all the cations present in the solution complicates the matter. Preferential attraction of cations to the layer depends on concentration, physical size and electrical charge (Huang et. al. 1988).

The selectivity of the separation process in a precipitate system is mainly caused by the selective aggregation of particles. The selectivity in the aggregation process resulted from differences in the non-electrostatic interactions between the particles, such as the van der Waals interaction.

Hee et. al. (2006) reported that hydration effects and osmotic effects due to (charged) surface groups that extend out into the solution (brushes) are the cause for the additional repulsive force shown in Fig.5.15. They suggested that steric repulsion between molecules on the particle surfaces, which is called brush repulsion, should be taken into account. They proposed the following mechanisms for binding: (1) the correlation of dipoles due to domain formation of an adsorbed surfactant film (2) non-uniform charge distribution on net neutral charged surfaces

(3) nucleation of air bubbles on the surface and (4) structural effects due to ordering of water molecules.

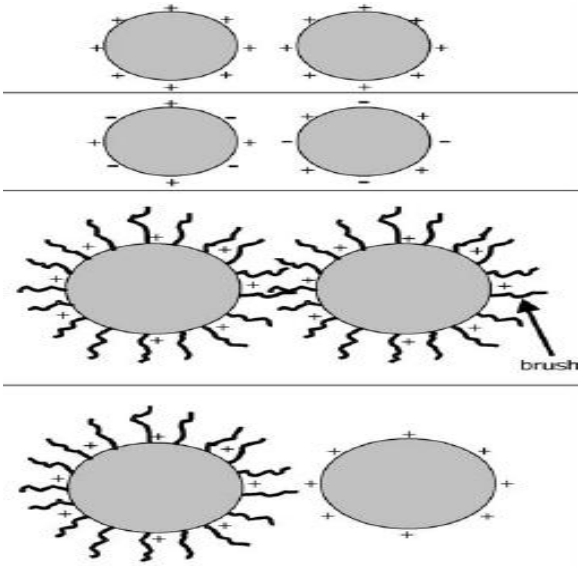

Fig. 5.15: Overview of interaction between particles

Particle–particle, particle–bubble interactions, van der Waals, electrostatic, brush repulsion and the so-called hydrophobic interactions are to be considered in selective metal removal. The latter two interaction forces are essential for describing the aggregation behaviour.

5.7.1 Zinc-Cadmium removal by foaming

Zinc-cadmium recovery was investigated on the same lines as that of individual metal cations investigated earlier and effect of pH was studied for fixed feed concentration of 100 ppm cadmium and 100 ppm zinc. Feed solution (450 ml) was charged in the column and foam samples were withdrawn from sample port O-3 that was located 157.5 cm above the initial liquid level. Air flow rate was maintained at 0.06 lpm. For individual metal cation removal it was observed that metal: SDS molar ratio 1:2 resulted in highest metal recovery for both Zn as well as Cd systems. However, in binary operation the metal: SDS molar ratio could not be balanced for both the cationic species, therefore the surfactant concentration was maintained at a constant value of 0.0030 gmmol/lit that corresponded to molar ratio of 1: 1.2. Total operational time was 20 minutes.

5.7.2 Effect of pH on zinc - cadmium removal

The speciation nature of cadmium sulfate and zinc sulfate in water corresponding to 100 ppm of cadmium and 100 ppm nickel in the initial feed concentration is shown in *Fig. 5.16* obtained using the Visual Minteq 2.15 software. Species formation reactions for individual metals were discussed in sec. 5. 4 and 5.5.

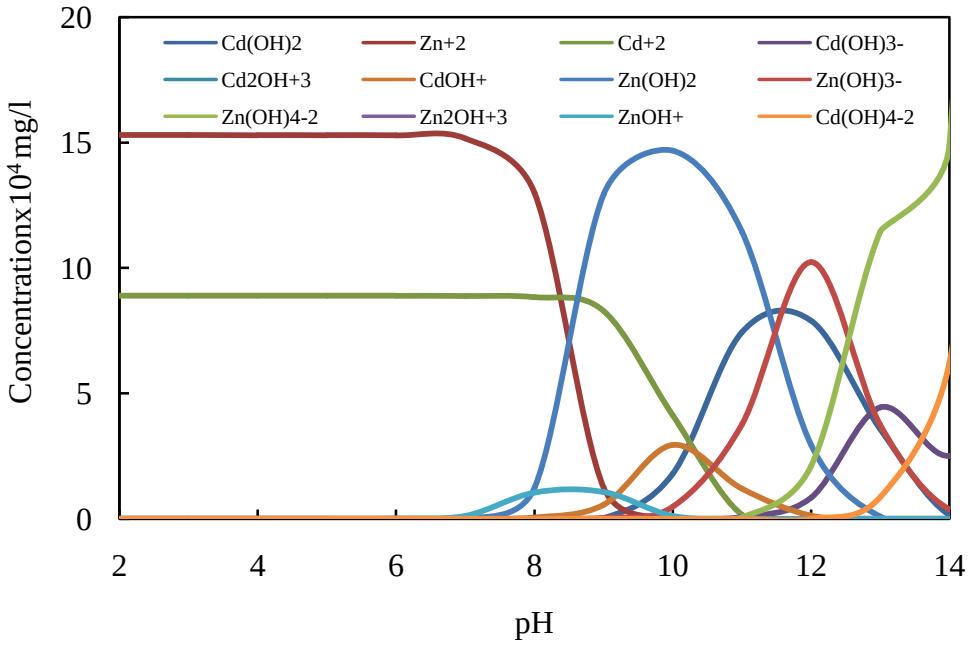

Fig. 5.16: Species distribution of 100 ppm cadmium and zinc each in water

The speciation was calculated as a function of pH. The fraction of cadmium species such as Cd^{2+} , $Cd(OH)^{+}$, $Cd(OH)_2$, $Cd(OH)_3^-$ and $Cd(OH)_4^{2-}$ in solution varies over a range of pH . Cd^{2+} is the main ions present in solution for pH < 9. Above pH 9 in basic conditions most Cd is present as $Cd(OH)_2$. At pH 11 $Cd(OH)_3^{2-}$ formation begins while at pH 12 or above the main cadmium specie is $Cd(OH)_4^{2-}$.

Polynuclear cadmium complex such as $Cd_2(OH)_3^+$ are also present. The zinc ion, Zn^{2+}, is the dominant specie up to pH 9 while zinc hydroxide, $Zn(OH)_2$ is the dominant species from pH 9 to pH 11. Above pH 10, $Zn(OH)_3^-$ formation occurs and above pH 11, $Zn(OH)_4^{2-}$ formation takes place.

The effect of solution pH on zinc and cadmium removal along with accompanying foamate volumes is shown in Fig. 5.17. Maximum zinc recovery of 34% was

obtained at pH 4, cadmium recovery of 83% was obtained at pH 4 which also corresponds to the maximum foamate volume obtained. The profile of foamate volume and zinc cadmium recovery follows similar pattern. This pattern of metal recovery could be attributed to ion-adsorption, the adsorption of Cd^{2+} ions and Zn^{+2} ions on SDS molecule leads to the transport of Cd-SDS and Zn-SDS complex with the ascending bubbles of the foam that tends to carry the Cd^{2+} ions and Zn^{2+} from feed to foamate.

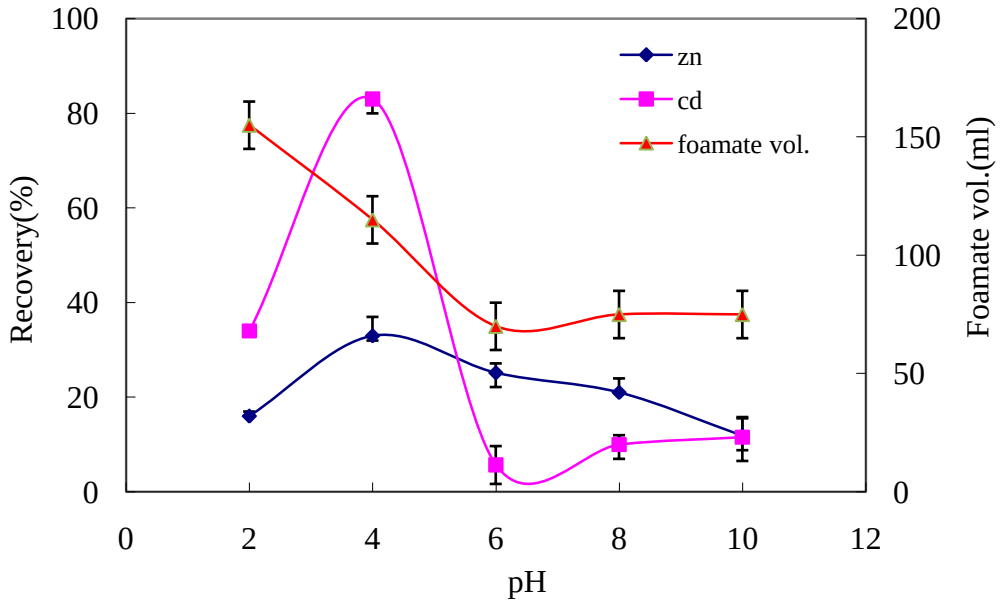

Fig. 5.17: Zn-Cd recovery and foamate volume vs pH for 100 ppm zinc and 100 ppm cadmium

The pattern of foamate surfactant concentration justifies that metal adsorbed on the surfactant is carried in foamate since increasing metal removal coincides with increasing surfactant concentration in foam. Cadmium recovery was just 5.7% and zinc recovery was 25.17 % at pH 6. Values of lower extent of zinc and cadmium recovery were attributed to competition of hydrogen ions with the metal cations for the available surfactant sites.

Till pH 8 Cd^{2+} and Zn^{2+} ion flotation is considered to be the cause of metals recovery. Significant concentration of hydrated precipitate of cadmium $Cd(OH)_2$, and $Zn(OH)_2$ are formed at pH > 9 which is confirmed by specie distribution diagram of 100 ppm cadmium and 100 ppm zinc in aqueous media. Fig. 5.18 shows metal removal and associated foamate surfactant concentrations at various pH values ranging between 2-10 for zinc-cadmium binary system.

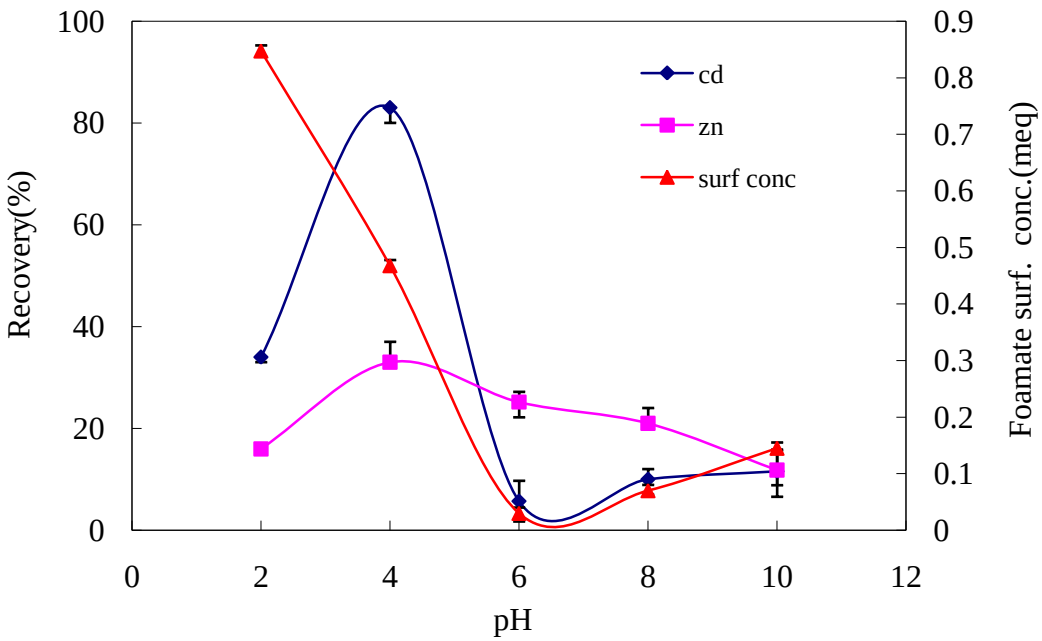

Fig. 5.18: Zn-Cd recovery and foamate surfactant concentration vs pH for 100 ppm zinc and 100 ppm cadmium

Cadmium separation is more at pH 4 compared to the similarly charged zinc species indicating a higher affinity of the cadmium species towards the SDS ions till pH 4.

5.7.3 Nickel-Cadmium removal by foaming

Nickel-cadmium recovery was also investigated in the same foam column FC-1 and the effect of pH was investigated for fixed feed concentration of 100 ppm nickel and 100 ppm cadmium. Feed solution (450 ml) was charged in the column and foam samples were withdrawn from sample port O-3 that was located 157.5 cm above the initial liquid level. Air flow rate was maintained at 0.06 lpm. SDS concentration of 0.0034 gmmole/lit was used in binary system of Ni-Cd mixture, corresponding to molar ratio of metal ion: surfactant 1:1.3. Total operational time was 20 minutes.

5.7.4 Effect of pH on nickel - cadmium removal

The speciation nature of nickel sulfate and cadmium sulfate in water corresponding to 100 ppm of cadmium and 100 ppm of nickel i.e the initial feed concentration is shown in *Fig. 5.19* obtained using the Visual Minteq 2.15 software. Species formation reactions for individual metals were discussed in sec. 5. 5 and 5.6

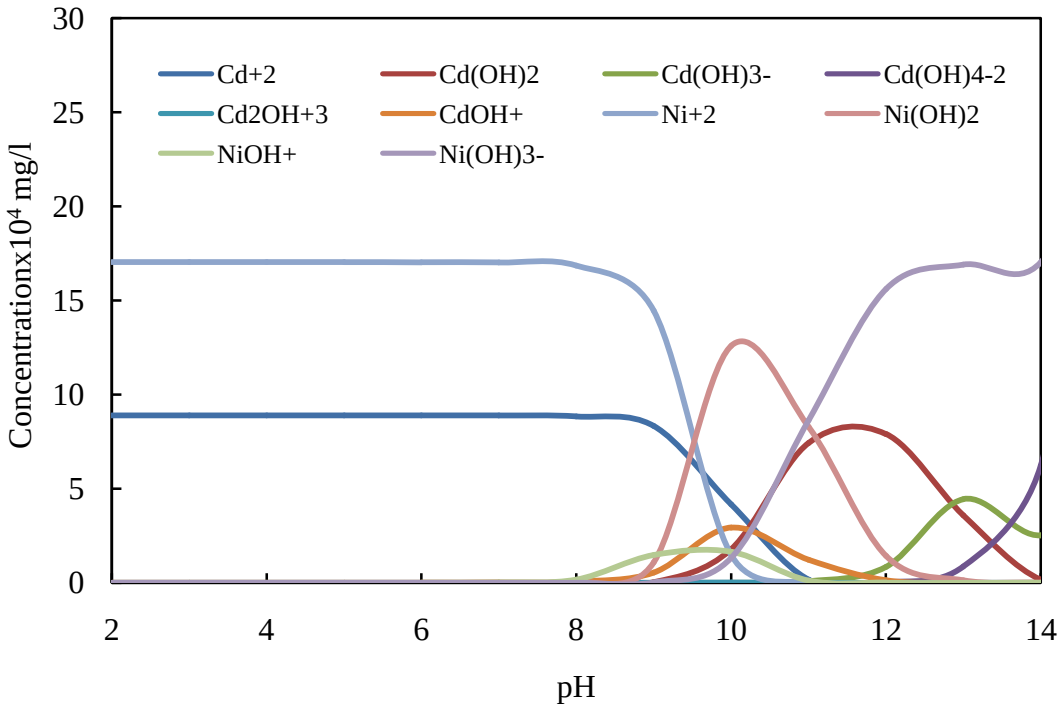

Fig. 5.19: Species distribution of nickel and cadmium (100 ppm each) in water

The speciation was calculated as a function of pH. The fraction of nickel species such as Ni^{2+}, $Ni(OH)^{+}$, $Ni(OH)_2$ and $Ni(OH)_3^{-}$ in solution varies over a range of pH. Ni^{2+} is the main ion present in solution till pH 8. Above pH 9 in basic conditions most Ni is present as $Ni(OH)_2$. $Ni(OH)_3^{2-}$ formation starts at pH 9 and at pH 12 or above, the main nickel specie is $Ni(OH)_3^{2-}$. $Ni(OH)^{+}$ formation also starts at pH 8.

The fraction of cadmium species such as Cd^{2+} , $Cd(OH)^{+}$, $Cd(OH)_2$, $Cd(OH)_3^{-}$ and $Cd(OH)_4^{2-}$ in solution varies over a range of pH . Cd^{2+} is the main ions present in solution for pH < 9. Above pH 9 in basic conditions most Cd is present as $Cd(OH)_2$. $Cd(OH)_3^{-}$ formation starts at pH 11 while at pH 12 or above, the main cadmium specie is $Cd(OH)_4^{2-}$. Polynuclear cadmium complex such as $Cd_2(OH)_3^{+}$ is also present.

The effect of solution pH on nickel-cadmium removal along with accompanying foamate volumes is shown in Fig 5.20 .Maximum cadmium recovery 23.59% was obtained at pH 6 with foamate volume 65 ml. Nickel recovery 55.72% was obtained at pH 10 which corresponds to the maximum foamate volume observed 171 ml. The profile of foamate volume and nickel-cadmium recovery follows the

same pattern. This pattern of metal recovery is attributed to ion-adsorption, the adsorption of Cd^{2+} ions and Ni^{+2} ions on SDS molecule leads to the transport of Cd-SDS and Ni-SDS complex with the ascending bubbles of the foam that tends to carry the Cd^{2+} ions and Ni^{2+} from feed to foamate.

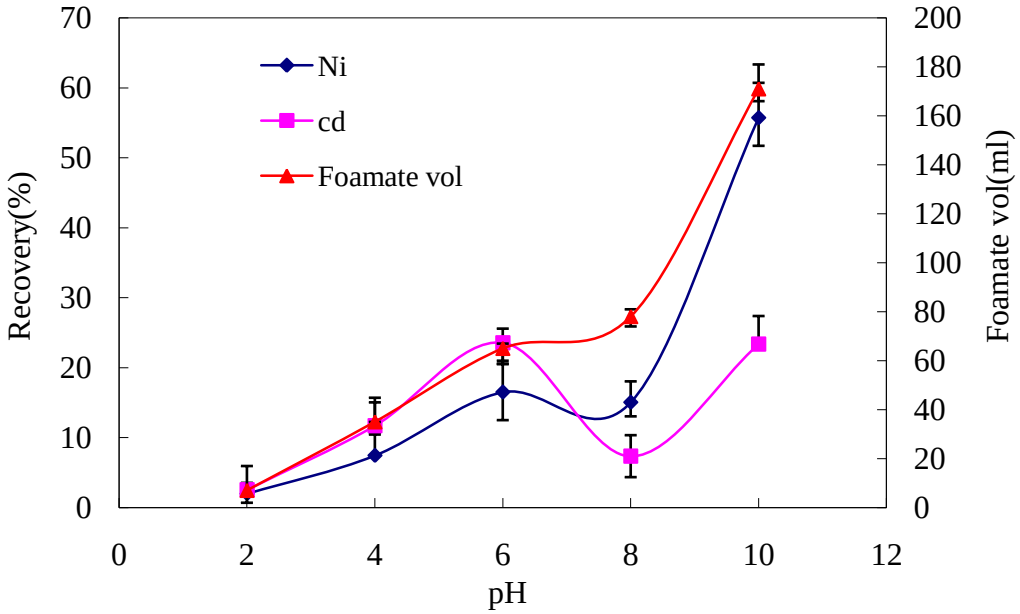

Fig. 5.20: Ni-Cd recovery and foamate volume vs pH for 100 ppm nickel and 100 ppm cadmium

Cadmium recovery was just 11.71% and nickel recovery was 7.45% at pH 4 where the collected foamate volume was 35 ml. Uptill pH 8 Cd^{2+} and Ni^{2+} ion flotation is considered to be the cause of metals recovery. Significant concentration of hydrated precipitate of cadmium $Cd(OH)_2$, and $Ni(OH)_2$ are formed at pH > 9 which is confirmed by specie distribution diagram of cadmium sulfate and zinc sulfate.

Figure 5.21 shows metal removal and associated foamate surfactant concentrations at various pH ranging between 2-10 for nickel-cadmium binary system. The foamate surfactant concentration is high when the metal recovery in the foamate is poor. For higher metal removal lower is the amount of surfactant obtained in foamate and vice versa, indicating removal by hydraulic entrainment.

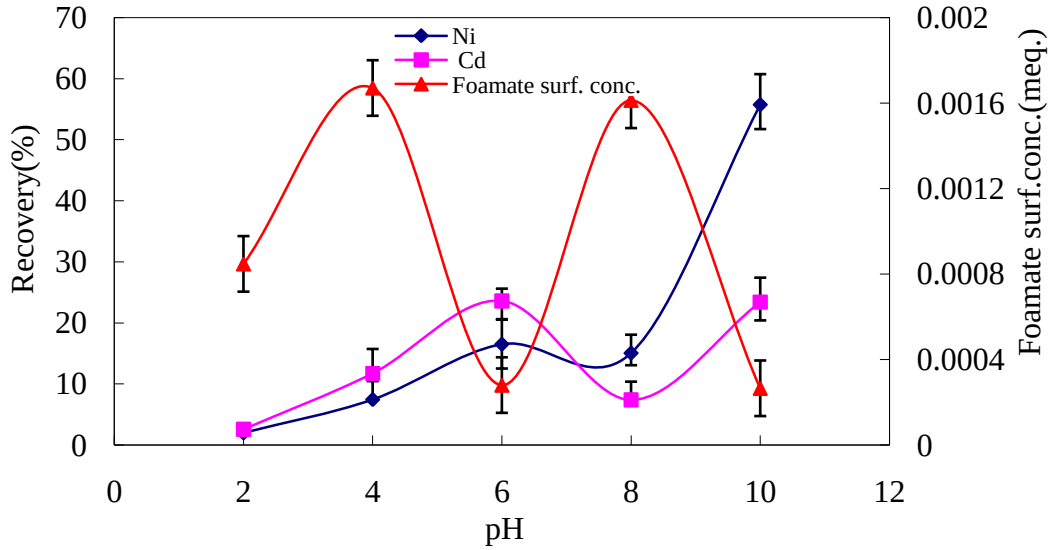

Fig. 5.21: Ni-Cd recovery and foamate surfactant concentration vs pH for 100 ppm nickel and 100 ppm cadmium

Cadmium recovery is higher till pH 6 that is the favorable condition for cadmium removal. The fact that cadmium removal is much more at these pH of 2, 4, 6 compared to the similarly charged nickel species is an indication of a higher affinity of the cadmium species towards the SDS molecules till pH 6. Higher Ni removal is at pH 8 and 10 indicates metal removal is in hydroxides form.

5.8 Flotation rate constant

The performance of a foam separation process is often expressed by a flotation rate constant that is defined as the first order rate constant, *ki*, for the change of particle concentration in time.

$$dn_i/_{dt} = -k_i n_i \qquad 5.7$$

Where ni is the concentration of particle type i in the suspension (m^3), t is time (sec) and ki is the effective flotation rate constant of particle type i (1/sec).

Particle–particle separation using flotation requires a difference in flotation rate constants for the different particles that need to be separated, so that their enrichment at the air–water interface is unequal. The flotation rate constant is influenced by particle–bubble interactions and hydrodynamic effects that are governed by particle size and momentum, bubble size and bubble velocity.

According to Hee et.al. (2006) increase in particle size through particle aggregation can enhance the efficiency off the process. Particle aggregation thus is one of the key processes for selective flotation.

5.8.1 Flotation rate constant (k) for Zn-Cd system

In the mixed binary system Cd^{2+} and Zn^{2+} ions are flotated at pH 4 which differs from the removal of these ions individually. It is possible to separate Zn^{2+} ions from the binary system Zn-Cd by controlling pH. Competition between cadmium and zinc species is likely to occur for the available SDS sites. Fig. 5.22 shows flotation rate constant for zinc and cadmiun in zinc-cadmium binary system. The floatation rate constant k is sensitive to pH.

Cd^{+2} and Zn^{+2} concentration is more till pH 8. Zinc hydroxide and cadmium hydroxide is dominant specie between pH 8 to 10. Flotation rate constant for zinc at pH 4 is 0.00136 min^{-1} and for cadmium it is 0.0151 min^{-1}. The higher value of flotation rate constant indicates higher cadmium removal at pH 4.

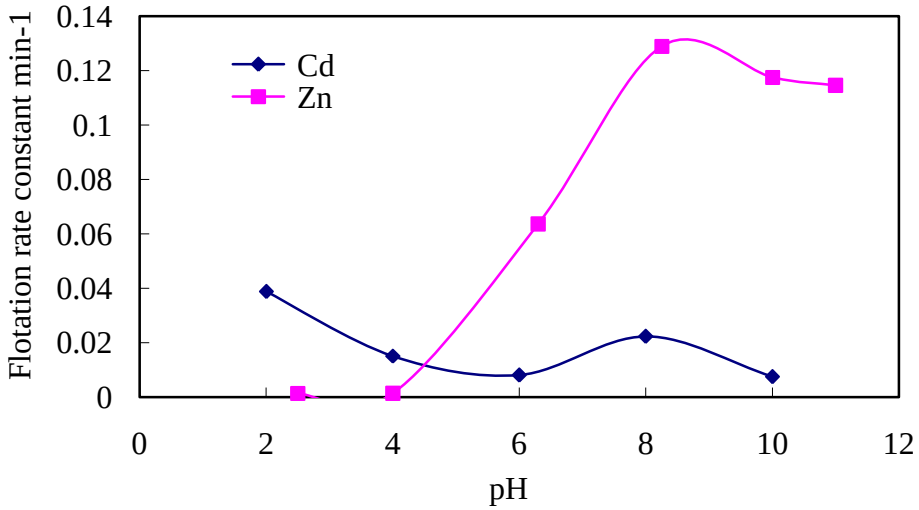

Fig. 5.22: Floatation rate constant vs pH for 100 ppm zinc and 100 ppm cadmium

Value of flotation rate constant is higher at pH 2 for cadmium compared to zinc . Removal of cadmium at pH 2 is also more compared to zinc. For zinc k is 0.129 min^{-1} at pH 8. For cadmium k is 0.02231 min^{-1} at pH 8. Zinc removal was 21% while cadmium removal was 10% at pH 8. After pH 6 zinc removal is more than cadmium as flotation rate constanst is also higher for zinc compared to cadmium after pH 6.

5.8.2. Flotation rate constant for Ni-Cd system

Competition between nickel and cadmium species is likely to occur for the available SDS sites. Cd^{+2} and Ni^{+2} concentration is more till pH 8 thereafter nickel hydroxide and cadmium hydroxide are the dominant specie between pH 8 - 10. Flotation rate constant for cadmium till pH 6 is more than for Ni. Recovery of metal also follows the same pattern.

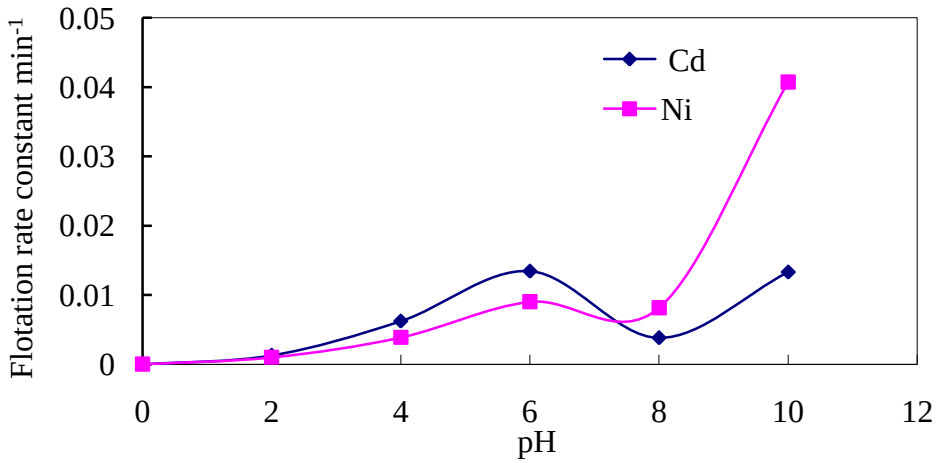

Fig. 5.23: Floatation rate constant vs pH for 100 ppm nickel and 100 ppm cadmium

Flotation rate constant is higher for nickel at pH 8 and pH 10. For pH 8 and 10 nickel removal is also higher than cadmium.

5.8.3 Utility of flotation rate constant

In general a first order model describes the flotation rates. This equation is expressed as follows:

$$R(t) = R_{\infty}(1 - e^{-kt}) \qquad 5.8$$

where R is the recovery at time t, R_{∞} is the ultimate recovery for an infinite time, and k is flotation rate constant (Polat 2000). Such kinetic equations predict the extent of recoveries for the floatation of hydrophobic particles having constant floatability.

Recovery of metal from feed at any time at a given pH was calculated by evaluating the flotation rate constant 'k' from experimental data. Cumulative recovery could also be calculated. Fig. 5.24 shows percentage of zinc removal at

every minute till 20 min. in the pH range of 2.5 to 10. This indicates that percentage removal increases with time. We can also predict time for maximum removal of metal. The recoveries were also verified experimentally for intermediate time intervals.

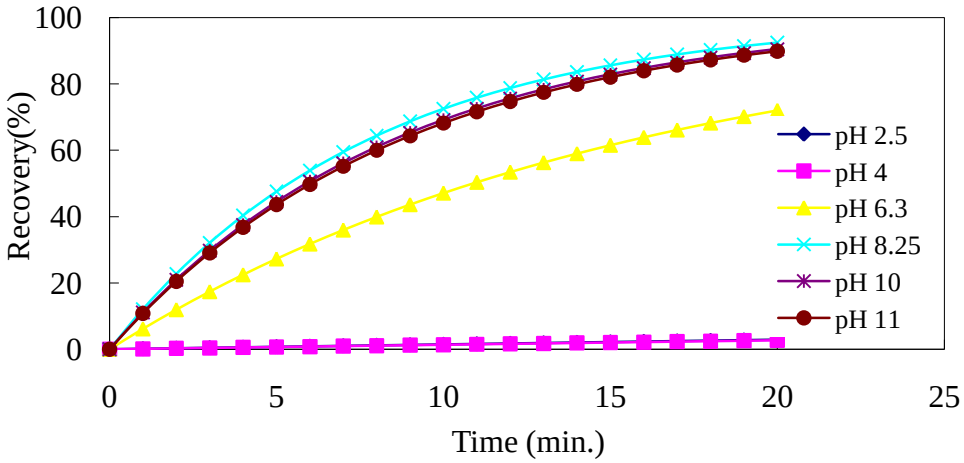

Fig. 5.24: 100 ppm zinc removal till 20 min. at 0.06 lpm for various pH

Cadmium removal at intermediate time can also be obtained for 100 ppm nickel metal at 0.06 lpm for varying pH between 2-10 which is shown in Fig. 5.25.

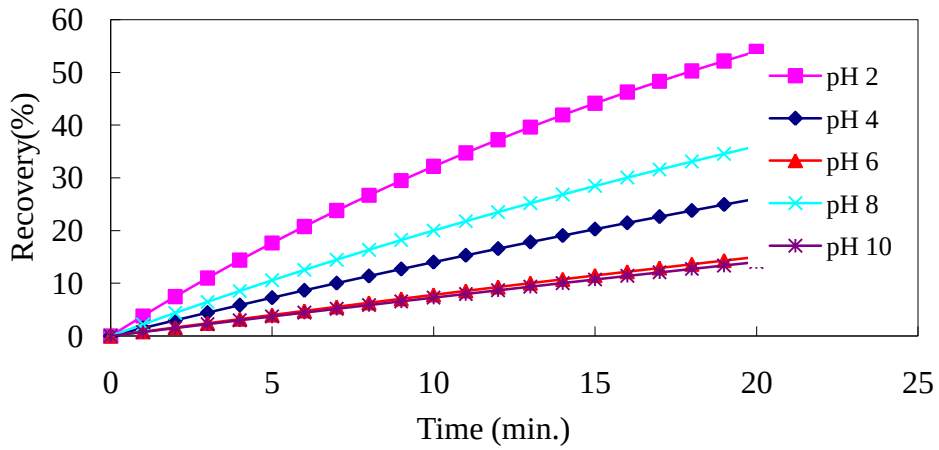

Fig. 5.25: 100 ppm cadmium removal till 20 min. at 0.06 lpm for various pH

Cadmium removal was 17.63 % for 5 min, 32.15% for 10 min, 44.12% for 15 min and 54% for 20 min. at pH 2 which was optimum pH for cadmium removal.

Nickel removal at intermediate time can also be obtained for 100 ppm nickel metal at 0.06 lpm for varying pH between 2-10 which is shown in Fig. 5.26.

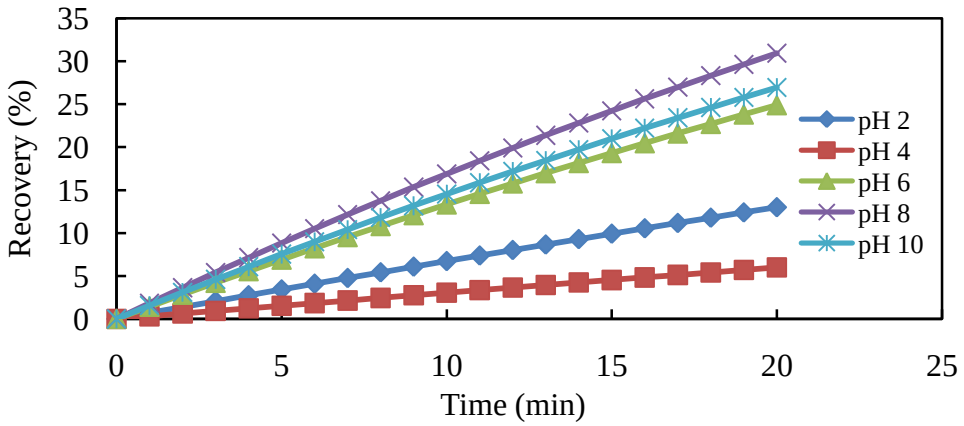

Fig. 5.26: 100 ppm nickel removal till 20 min. for 0.06 lpm at various pH

Nickel removal was 8.83 % for 5 min , 16.88% for 10 min , 24.23 % for 15 min and 30.92% for 20 min. at pH 8 which was optimum for nickel removal.

5.9 Evaluation of the Distribution factor

Application of foaming to the removal of non surface active species requires a method of specificity of the foam surface for individual ions in solution. This specificity may arise from charge interactions between the adsorbed surfactant layer and a diffuse double layer of counter ions or bonded interactions between surfactant and metal ions. Competitive coadsorption of ions of opposite charge to the surfactant based on diffuse double layer theory allowing for the differences in the distance of closest approach of ions of different size has been discussed by Huang and Talbot (1973). This theory facilitates one to predict the distribution factor of each species between a solution of mixed electrolyte and a surface layer.

The evaluation of distribution coefficient assumes that the column is one theoretical stage and the liquid pool is well mixed it is assumed that bubbles are spherical and uniform and there is no coalescence in the rising foam. Mass balance on the collapsed foam indicates

$$D = \frac{Q}{S}\left(\frac{n_f}{n} - 1\right) \qquad 5.9$$

Where, n_f = Foamate concentration moles/l

n= Bulk concentration moles/l,

D= Distribution factor cm

S is the surface rate generated which can be estimated by S= r N π d^2

r = Openings in sparger

N= Bubble emission frequency (bubbbles/mim)

d= Diameter of individual bubble (cm) where $d= (6G/ r N \pi)^{1/3}$

G= Volumetric gas rate (cm^3/min)

Q= volumetric rate of foam overflow on a gas free basis

Average bubble size and bubble counts/min were evaluated using photographic technique and these captured images were analyzed using the Image J software. The surface generation rate S was conveniently calculated by multiplying the (number of counts/min) with the average bubble size. Presence of metal in feed prepared (n) and foamate concentration (n_f) were evaluated by metal analysis using AAS. Volumetric rate of foam overflow was (cm^3/min) was evaluated experimentally. The results calculated for the various runs are listed in Table 5.2

Table 5.2: Distribution factors calculated for metals at various pH

pH	Nickel		Cadmium		Zinc	
	D cm	Recovery %	D cm	Recovery %	D cm	Recovery %
2	$2.7x10^{-6}$	13	$6.56x10^{-3}$	54	0.4439	2.8
4	$2.18x10^{-3}$	06	$-5.63x10^{-5}$	26	-0.018	2.7
6	-0.0169	25	$5.83x10^{-3}$	15	0.1280	72
8	$-4.56x10^{-3}$	31	0.01582	36	0.071	92.43
10	$-2.61x10^{-3}$	27	$-7.739 x10^{-3}$	14	0.075	90.5

Results indicate that for nickel removal pH 6-10, for cadmium removal pH 4 & 10 and for zinc removal at pH 4 the distribution factors are negative which is meaningless making these results unacceptable. The plausible reasons for such behavior are the following :-

(i) Metal removal is not due to ion adsorption mechanism but due to hydraulic entrainment.

(ii) Production of polyhdroxyl and polynuclear complexes takes place as pH increases.

More focused work is required to gain deeper insight in the relation between selectivity and distribution factor.

5.10 Effect of surfactant polymer interaction on metal removal

Water soluble polymers are incorporated in aqueous surfactant solutions in many domestic and technological applications. Polymers are added as viscosity modifiers and as stabilizers. Water soluble polymers often interact strongly with surfactants in aqueous solution. This gives rise to change in surface tension.

5.10.1 Cadmium removal using SDS-PVP complex

The foaming behavior of the anionic surfactant SDS was studied in the presence of nonionic polymer poly(vinylpyrrolidone) (PVP) and reported in Chapter 4. The effect of presence of PVP (1% wt) on cadmium removal was investigated for pH values ranging between 2-10.

Cadmium recovery was investigated from sample port O-3. Feed volume of 450 ml containing 100 ppm cadmium having Cd:SDS 1:2 molar ratio along with (1% wt) PVP for 20 min time and 0.06 lpm air flowrate was charged to glass column. Fig. 5.27(a) shows the influence of solution pH on cadmium removal in presence of surfactant-polymer SDS-PVP along with collected foamate volumes. Maximum removal 61% was obtained at pH 8.

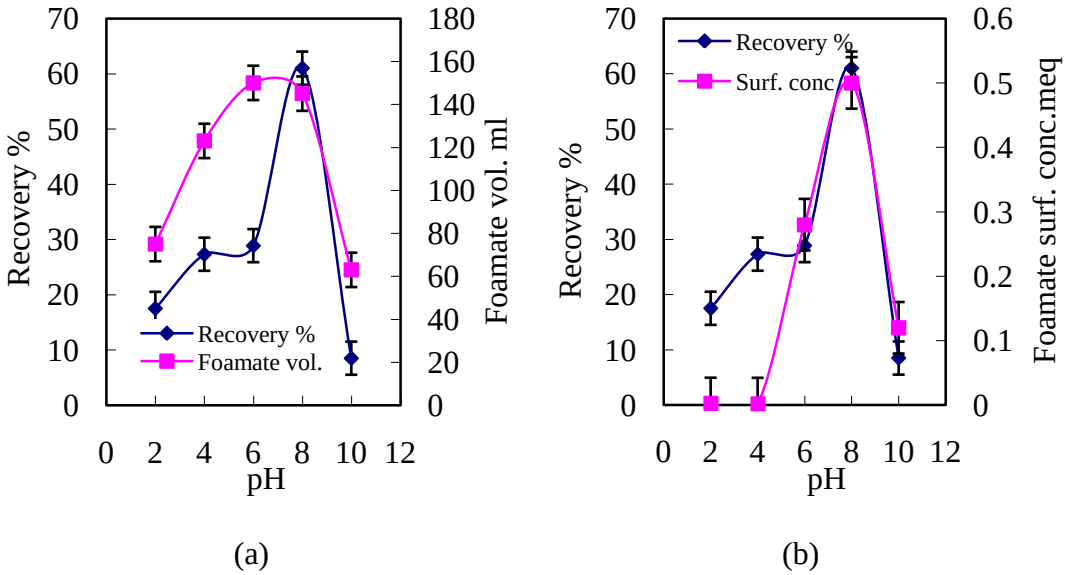

Fig. 5.27: (a) Effect of pH on percentage removal of cadmium and foamate volume in presence of PVP. (b) Effect of pH on percentage removal of cadmium and SDS concentration in presence of PVP

Foamate surfactant concentration obtained at pH 8 is also high shown in Fig. 5.27 (b). It justifies that metal adsorbed on the surfactant is carried in foamate. Cadmium precipitates as cadmium hydroxide above pH 6.

The interaction between SDS and SDS- PVP complex in solution is shown in Fig. 5.28. Most likely, the polymer shields the repulsive charges between the surfactant headgroups, thus lowering the free energy in forming the surfactant monolayer at the surface. Furthermore, shielding of the charges between the surfactant headgroups increases the critical packing parameters of the surfactants present at the surface. Thus the surfactants are able to pack more favorably at the surface, permitting more densely packed surfactant layer.

Fig. 5.28: Complex formation of SDS and PVP in bulk solution and at the liquid/air surface

There is complex formation at the surface between the surfactant and the polymer rendering lower metal removal. Cadmium recovery decreased to 17.5 % from 54 % at pH 2 in presence of polymer PVP as shown in Fig. 5.29(a) due to surfactant-polymer interaction.

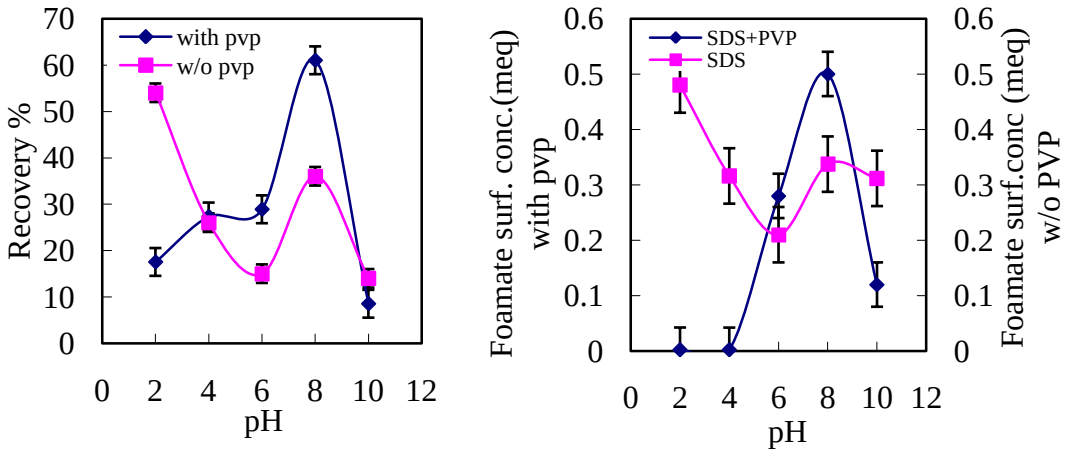

(a) **(b)**

Fig. 5.29: (a) Effect of pH on cadmium removal with and without PVP (b) Effect of pH on foamate surfactant concentration in absence and presence of PVP

The polarizable pyrrolidone side group in the polymer acquires positive charge on the ring nitrogen wherein an anionic surfactant sodium dodecyl sulfate (SDS) interacts (Prasad 2006), thus the anionic surfactants favorably interact with water-soluble polymers thereby declining the metal uptake.

Fig. 5.29(b) shows foamate surfactant concentration in presence and absence of PVP. Higher SDS concentration is obtained for higher cadmium removal which indicates strong association of surfactant with metal at specific pH.

5.11 Characterization of precipitates collected in foamate

The size, shape and elemental analysis of precipitates floated were performed by different instruments like SEM-EDX, particle size analyzer etc., Microscopy based techniques for particle size characterization provides powerful tool for characterization of particle size, size distribution and morphology. Scanning electron microscope enables examination at higher magnification and resolution. They are suitable for particles in the size range of about 0.1 µm to 1000 µm.

Foamate was collected for 100 ppm zinc having Zn:SDS 1:2 molar ratio for 20 min time and 0.06 lpm air flowrate from sample port O-3 at pH 8.25 where maximum zinc recovery was obtained. Under identical conditions foamate was collected for Cd at pH 2, Cd-PVP at pH 8 and for Ni at pH 8 where maximum metal recovery was obtained. Foamate collected was collapsed and centrifuged at 5000 rpm for 15 min. Upper liquid layer was decanted and the solid particles (sublate) settled at the bottom of test tube were washed repeatedly with water in order to remove SDS . Water washed particles were kept in petridish in oven for three hrs at 150 ^{0}C for drying and then in a dessicator for one day before analysis.

5.11.1 Fourier Transform Infrared Spectrometry (FTIR) for SDS and metals

IR spectroscopy is designed to measure vibration spectra and yield information pertaining to chemical bonds. It is based on molecular vibrations, accompanied by changes in the bipolar moment in the middle IR region and the wave number region between 4000 and 400 cm^{-1}.This mode of vibration includes bending/stretching, rotating, pinching, twisting and oscillating vibration and so on, which collectively cause intense IR absorption. The device often used for this

method is the Fourier transformation IR (FT-IR) spectroscope. With the FTIR, coherent light is usually applied to the sample via Michelson interferometer and the obtained interference signals are subjected to Fourier transformation.

Fig. 5.30 compares the infrared spectra of a) SDS b) zinc dodecyl sulfate c) cadmium dodecyl sulfate d) nickel dodecyl sulfate in the sulfate headgroup band region of 4000–400 cm^{-1}. The SO_2 asymmetric vibrational feature ((SO_2)) is the most intense band in the SDS spectrum. It is a combination of several overlapping peaks. As observed in Fig. 5.30 γas(SO_2) is located at 1249.91 and 1224.84 cm^{-1}. The separation between these two peaks is an indicative of the conformational structure. An important aspect about the SO_2 symmetric vibrational feature is its observation at 1084 cm^{-1}.

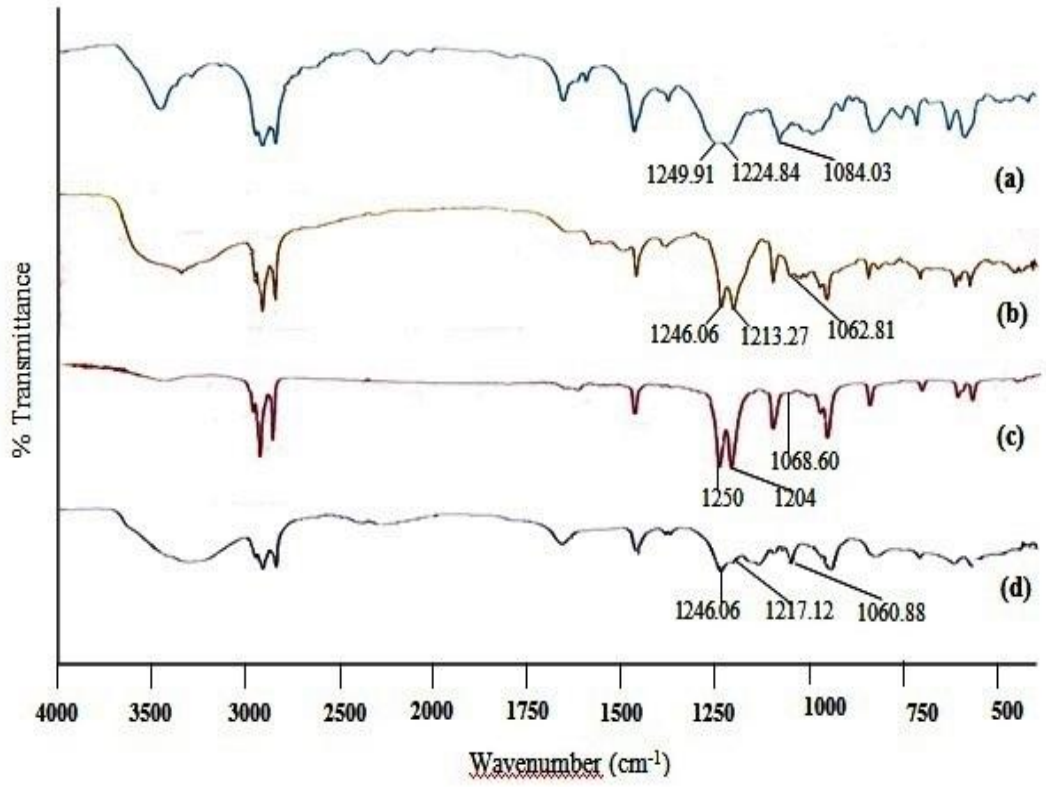

Fig. 5.30: FT-IR spectra of (a) SDS (b) zinc dodecyl sulfate (c) cadmium dodecyl sulfate (d) nickel dodecyl sulfate

The positions of the γas mode was 1246.06 cm^{-1} and the other γas and γs modes were significantly shifted to lower wavelengths of 1213.27 and 1062.81 cm^{-1} respectively for zinc dodecyl sulfate. The band shift is likely to be associated with an electrostatic effect involving coordination of the sulfate headgroup oxygen atom to zinc. The positions of the γas mode 1250 cm^{-1} were almost unchanged, but the

other γas and γs modes were significantly shifted to lower wavelengths of 1204 and 1068.60 cm^{-1} respectively for cadmium dodecyl sulfate.

The band shift is likely to be associated with an electrostatic effect involving coordination of the sulfate headgroup oxygen atom to cadmium. The positions of the γas mode was 1246.06 cm^{-1} and the other γas and γs modes were significantly shifted to lower wavelengths 1217.12 and 1060.88 cm^{-1} respectively for nickel dodecyl sulfate. The band shift is likely to be associated with an electrostatic effect involving coordination of the sulfate head group oxygen atom to nickel.

5.11.2 SEM/EDX of zinc dodecyl sulfate

Scanning electron microscopy is the technique in which the electron microscope images a sample with the beam of electrons. The electrons will interact with the atoms of the sample producing the signals that contains the information about structure, morphology and particle size of the sample.

Energy dispersive X-ray spectrum analysis is an analytical technique used for the elemental analysis of the sample. It depends on the interactions of the X-ray with the sample. Each element has a unique atomic structure which allows a unique set of peaks on its X-ray spectrum.

Foamate was collected for a feed concentration of 100 ppm zinc floated at pH 8 for 20 min time and 0.06 lpm air flowrate. Foamate was collected from sample port O-3 where maximum zinc recovery was obtained. Foamate collected was collapsed and centrifuged at 5000 rpm for 15 min.

Upper liquid layer was decanted and the solid particles (sublate)of zinc dodecyl sulfate settled at the bottom of test tube were washed repeatedly with water in order to remove SDS. Water washed particles of zinc dodecyl sulfate were kept for drying in a petridish in an oven at 150^0 C for three hours and then in a dessicator for one day.

Fig.5.31 (a) presents the morphology and Fig. 5.31(b) presents energy dispersive X-ray spectrum of the zinc dodecyl sulfate. The structure is fibrous.

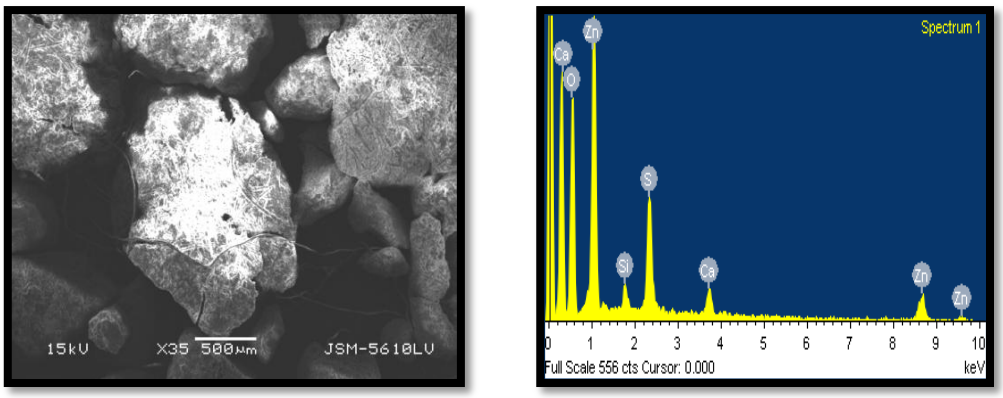

(a) **(b)**

Fig. 5.31: (a) SEM and (b) EDX of formed zinc dodecyl sulfate

The weight percentage of Zn and S were 44.62% and 10.55% respectively which indicates the formation of zinc dodecylsulfate. The peaks at 1, 8.5 and 9.5 keV were due to zinc.

5.11.3 X-Ray diffraction of zinc dodecyl sulfate

X-Ray diffraction (XRD) method characterizes crystal structures. XRD measurement is important to identify the main component of material. The powder XRD method is especially suitable for evaluating crystalline size. It is based on the intensity of an X-ray hitting a sample as a function of the scattered angle, polarization, wavelength or energy. XRD of zinc dodecyl sulfate is shown in Fig. 5.32

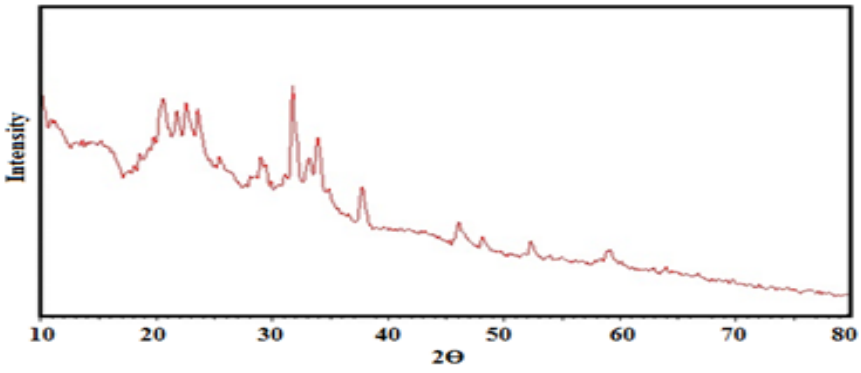

Fig. 5.32: XRD profile of zinc dodecyl sulfate

The X-Ray powder of diffraction pattern of SDS exhibited characteristic peaks at 20.59, 20.83 which revealed the presence of some crystallinity. Similar results were observed by Bhise et al. 2009 also. XRD of zinc dodecyl sulfate showed

presence of 18.7% zinc sulfate orthorhombic, 4.1% Zinc sulfite and monoclinic SDS. Details of XRD profile of zinc dodecyl sulfate are shown in Appendix B.

5.11.4 Particle size distribution of zinc dodecyl sulfate

Knowledge of particle sizes and the size distribution is prerequisite for most processing operations. The particle size distribution of a material is important in understanding its physical and chemical properties. To represent three dimensional particle in one dimension the term "particle size" is used. Regular particles have a definite shape but for the irregular particles equivalent size is used.

The particle size and size distribution of the particles were obtained by using Mastersizer 2000 MU (Malvern Instruments) using water as the dispersant. It uses the technique of laser diffraction to measure the sizes of particles. It does this by measuring the intensity of light scattered as the laser beam passes through the dispersed particulate sample. This data is then analyzed to calculate the size of the particle that created the scattering pattern.

During zinc removal experiments particles are seen in collected foamate at pH 8.25 where maximum zinc removal was obtained. To study the size of formed particles in foamate and effect of surfactant SDS on particle size different feeds were prepared.

In first case prepared feed contains 100 ppm zinc at pH 8.25. Formed zinc hydroxides were evaluated for particle size anaylsis.

In second case prepared feed contains 100 ppm zinc and SDS having Zn:SDS 1:2 mole basis. pH was adjusted to 8.25 and formed hydroxide precipitates were analyzed . For this case the feed with same composition was charged in glass column at 0.06 lpm for 20 min. and obtained foamate of zinc dodecyl sulfate was analyzed for particle size.

For third case prepared feed contains 100 ppm zinc with Zn:SDS 1:4 mole basis pH was adjusted to 8.25 and formed hydroxide precipitates were analyzed . For this case the feed with same composition was charged in glass column at 0.06 lpm

for 20 min. and obtained foamate of zinc dodecyl sulfate was analyzed for particle size.

Fig. 5.33 shows the particle size analysis of foamate after 24 hr and 25 ^{0}C. The particle sizes are influenced by the nature of the associated anion, introduction of higher quantity of SDS led to drastic size reduction.

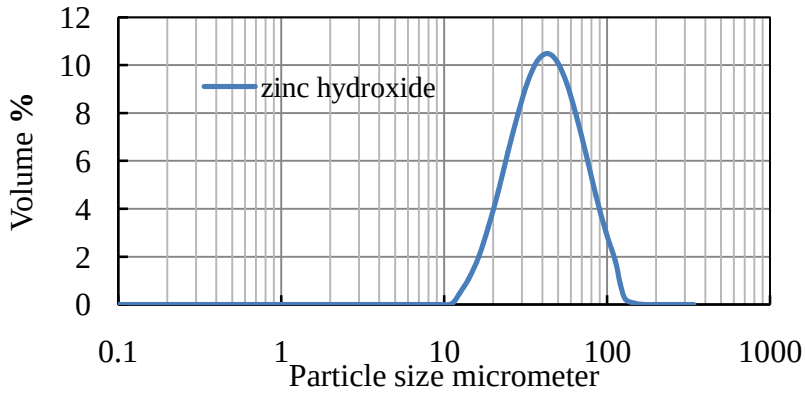

(a)

Fig. 5.33(a): Particle size distribution of feed for Zn:SDS 1:2 at pH 8.25

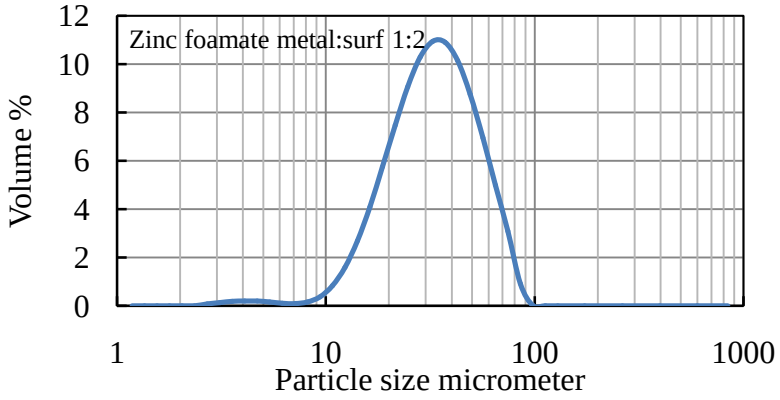

(b)

Fig. 5.33 (b): Particle size distribution of foamate for Zn:SDS 1:2 at pH 8.25

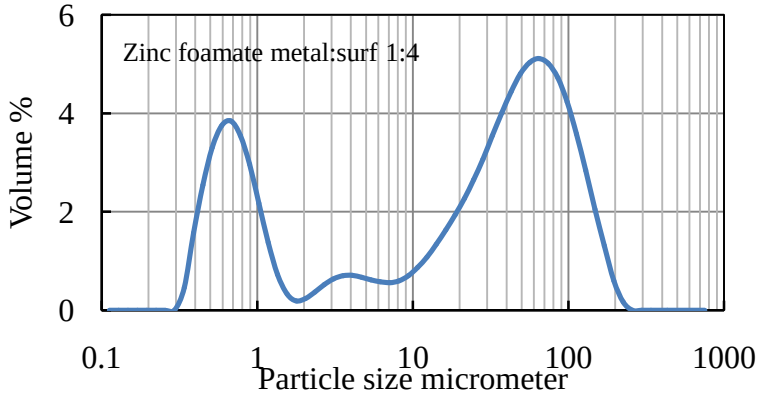

(c)

Fig. 5.33(c): Particle size distribution of foamate for Zn:SDS 1:4 at pH 8.25

By increasing the surfactant quantity particle growth was arrested. The complexing attachment phenomena of the zinc hydroxide particles with SDS lead to the arrest of particle growth processes. Similar results were reported by Oliveira et. al. (2003) also.

The presence of higher surfactant SDS significantly decreased crystallite size. Size reduction occurs when surfactant molecules stick to some faces of crystallites. Particle size analysis of feed and foamate is shown in Table 5.3

Table 5.3: Particle size analysis of precipitates

Zinc hydroxide precipitate at pH 8.25	**d(0.1) µm**	**d(0.5) µm**	**d(0.9) µm**	**Spec. surface area m^2/g**	**D [3,2] µm**	**D [4,3] µm**
Precipitate collected in absence of SDS	21.964	42.309	80.657	0.169	37.339	47.579
Precipitate collected in feed Zn:SDS molar ratio 1:2	12.494	27.433	53.919	0.288	20.842	30.686
Precipitate collected in foamate Zn:SDS 1:2	9.178	30.3332	64.909	0.43	13.94	34.310
Precipitate collected in feed presence of excess of SDS Zn:SDS molar ratio 1:4	0.595	32.025	106.790	2.7	2.226	42.960
Precipitate collected in foamate in presence of excess of SDS Zn:SDS molar ratio 1:4	3.185	12.013	40.972	0.969	6.194	19.613

For precipitates collected in foamate of Zn:SDS1:2 molar ratio d(0.1), d(0.5) and d(0.9) obtained were 9.178, 30.33,64.909 respectively. For precipitates of foamate of Zn:SDS1:4 molar ratio d(0.1), d(0.5) and d(0.9) shifted to 3.185,12.013 and 40.972 respectively.

5.11.5 Sublate in foam column for cadmium removal

Feed 100 ppm cadmium and SDS having molar ratio 1:2 is charged in foam column (FC-1) under identical conditions discussed earlier .Foam initially consists of spherical bubbles.

Fig.5.34 shows that initially the foam height increases with the rate of foam generation. There is no rupture of films between the bubbles, except at the top so that the same bubble size is retained throughout column.

Foam is continuously generated in a column by addition of air bubbles from the liquid below. Sparging fixed amount of gas at a constant flow rate through a solution generate foam.

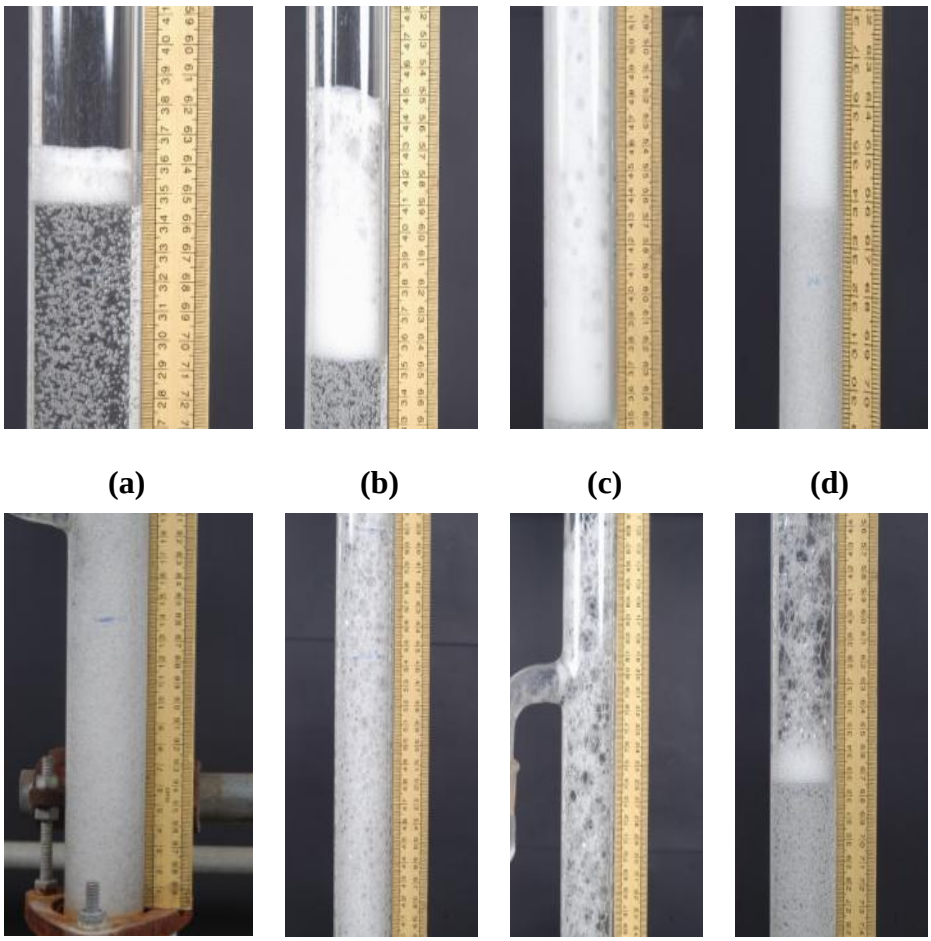

Fig. 5.34: Foam behaviour in column with increasing time.

Images were captured by photographic technique which shows sublalte captured in dry foam as shown in figure 5.35. As foam generated travels through column the liquid drains between adjacent bubbles, and their shape deforms. Drainage of liquid ultimately results in a polyhedral foam.

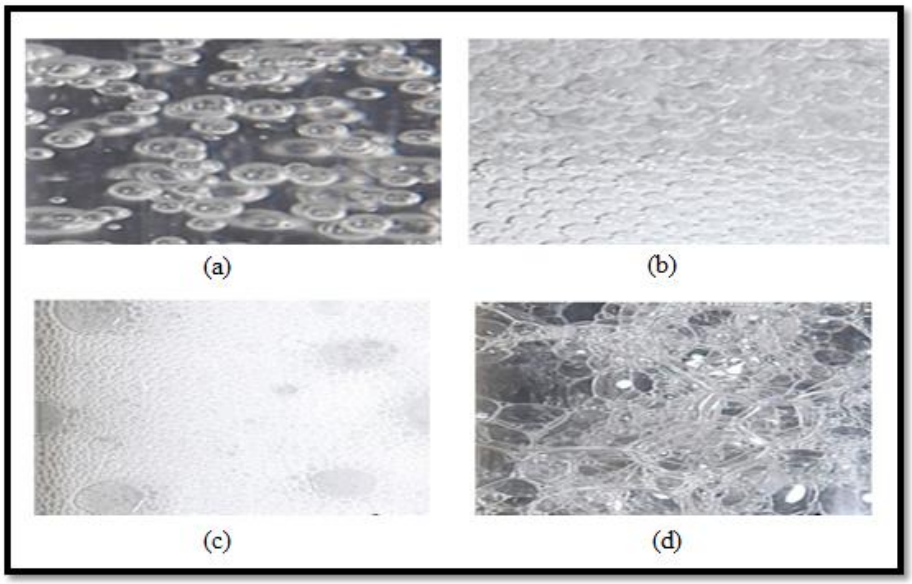

Fig. 5.35: Cadmium dodecyl sulfate captudred in foam(Cd:SDS 1:2mole basis)

5.11.6 SEM/EDX of cadmium dodecyl sulfate

Particles of cadmium dodecyl sulfate at pH 2 were separated as discussed in sec. 5.11.2. Particles were analysed for morphology and elemental analysis by SEM and EDX respectively. Fig. 5.36 (a), (b), (c) shows granular structure of cadmium dodecyl sulfate.

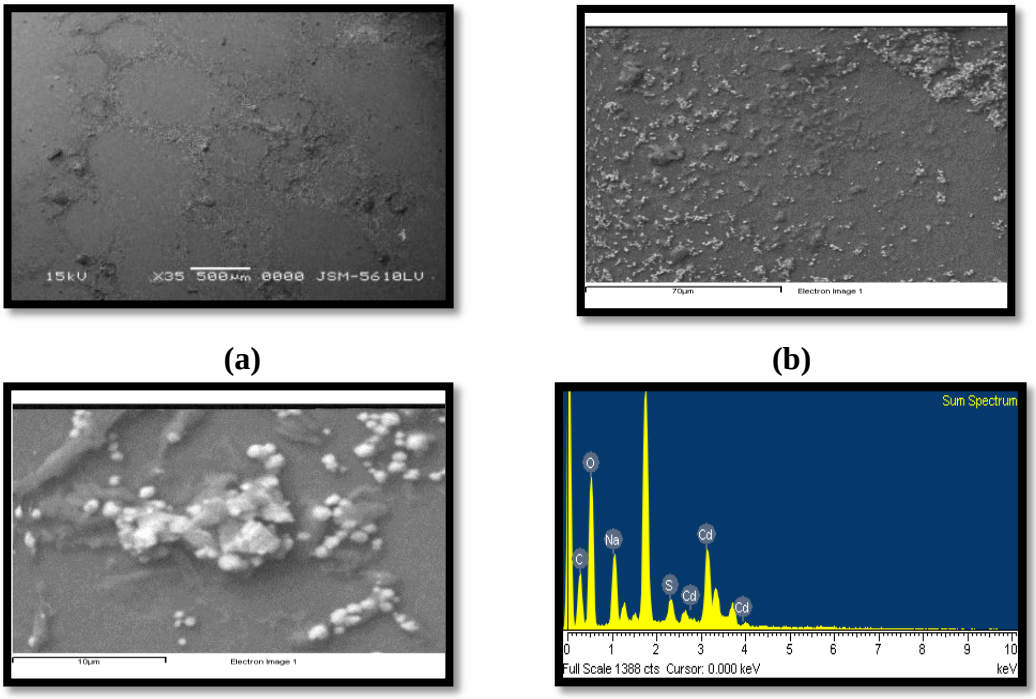

(a) **(b)**

(c) **(d)**

Fig. 5.36: SEM and EDX of formed cadmium dodecyl sulfate sulfate/Sodium dodecyl sulfate (a), (b), (c) SEM of sublate and (d) EDX of sublate

EDX showed Na indicating presence of SDS. The peaks at 2.8, 3 and 3.9 keV were due to Cd. The EDX indicates the formation of cadmium dodecyl sulfate.

5.11.7 SEM/EDX of cadmium dodecyl sulfate in presence of PVP

Particles of cadmium dodecyl sulfate at pH 8 in presence of 1% wt PVP were separated as discussed in sec. 5.11.2. Particles of sublate cadmium dodecyl sulfate in presence of 1% wt PVP were analyzed for morphology by SEM analysis.

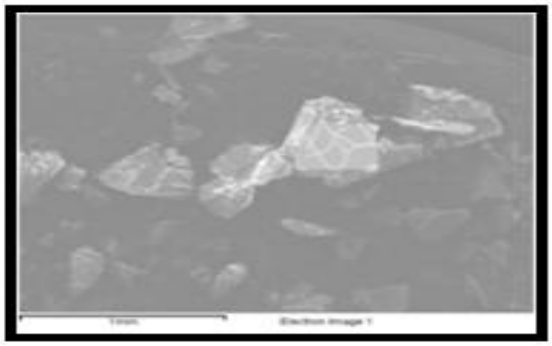

Fig.5.37: SEM of cadmium dodecyl sulfate in presence of 1% by wt PVP

Fig. 5.37 shows SEM image of cadmium dodecyl sulfate particles formed in presence of 1% by wt PVP. The formed particles have regular crystalline structure.

5.11.8 SEM/EDX of nickel dodecyl sulfate

Foamate was collected under identical conditions at optimum pH 8 for nickel. Nickel dodecyl sulfate was separated as discussed in sec. 5.11.2. and analysed for morphology and elemental analysis by SEM and EDX respectively. Fig. 5.38 (a), (b), presents the structure of the sublate which is in the form of thin filaments.

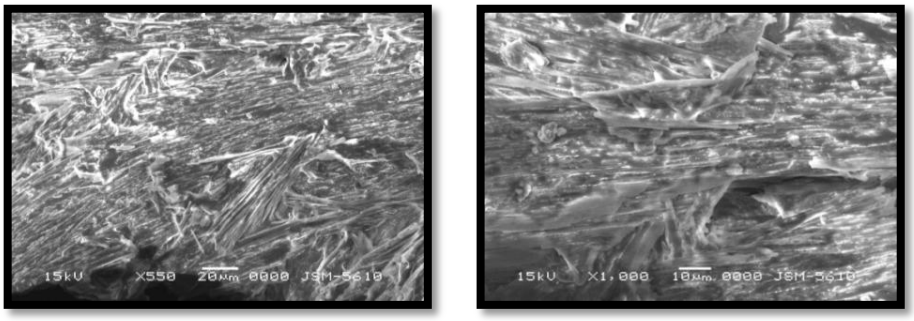

(a) **(b)**

Fig. 5.38: (a) , (b) SEM of the sublate nickel dodecyl sulfate

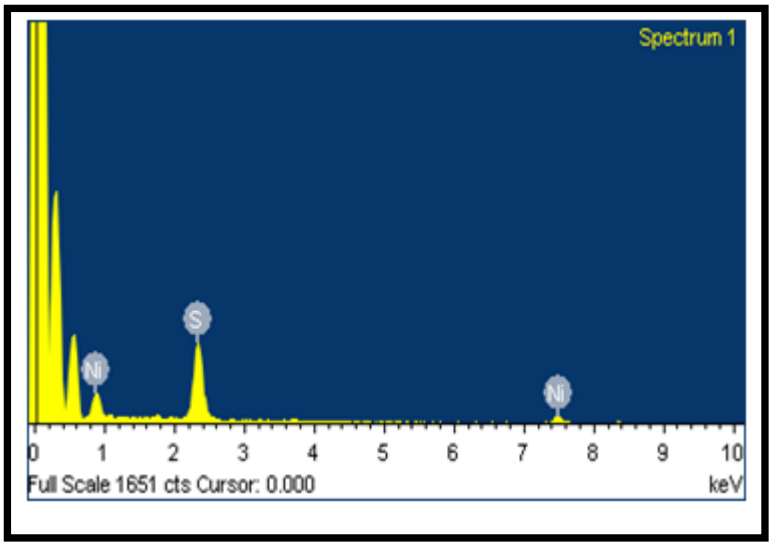

(c)

Fig. 5.38: (c) EDX of the sublate Nickel dodecyl sulfate

The weight percentage of Ni and S were 30.45% and 69.55% respectively which indicates the formation of nickel dodecy lsulfate. The peaks at 0.9 and 7.5 keV were due to nickel.

5.12 Scale up of column operations

To investigate the recoveries and foam behavior in larger diameter column a glass column having 10.16 cm diameter and 1 m height with multiple sample outlets was also fabricated as discussed in Chapter 3 (FC-3).

5.12.1 Effect of column diameter on foam behavior and removal of metals

To scale up and validate pattern of recovery data a larger diameter column of 10.16 cm i.d. was fabricated. To maintain dynamic similarity the superficial air velocity was kept constant in the prototype column and the larger diameter column i.e. Q/A in both columns was kept constant in view of this the air flow rate turned out to be 0.387 lpm in the 10 cm i.d. column. Feed volume used in the bigger column was 1125 ml. Recoveries were calculated for metals cadmium, zinc, nickel, cadmium-zinc, nickel–cadmium binary systems and cadmium-PVP systems at their optimum pH values. Foam obtained was quite dry at the top of the column at a distance of 1m.

Very dry foam was obtained at top of column for Ni:SDS 1:2 molar ratio . This

indicates the drainage was faster and not hindered.Fig.5.39 (a) shows dry foam and sublate nickel dodecyl sulfate captured in dry foam is shown in Fig. 5.39 (b).

(a) **(b)**

Fig. 5.39: (a) Dry foam and (b) nickel dodecyl sulfate captured in dry foam

Bubbles tend to set up a stable porous-type network inside the foam which is supported mechanically by its contact with the column walls. If the diameter of the column is larger the mechanical support of the walls may not be adequate to sustain the integrity of the foam structure and so the foam soon breaks down under its own weight.

Papara (2009) ascribed the fast foam decay in the large foam column to the relatively large distance between the walls and the central regions of the foam which does not allow adequate mechanical support of these regions and so the foam structure disintegrates under its own weight. This nature of foam indicates weak attachment of sublate to the bubble surface in foams.

The presence of solids tends to stabilize liquid films. One explanation for this is that surface active materials are adsorbed onto the solid particles, with non-polar ends oriented towards the water phase. This imparts a hydrophobic character to the particles, so that air bubbles adhere to them, resulting in a stabilization of the bubble and longer bubble survival time.

Two mechanisms have been suggested to explain the foam stabilization effects caused by particles adsorbed at the interface. The first effect results from a change

in capillary pressure. This is caused by the presence of adsorbed particles modifying the curvature of the g/l interface which reduces the pressure difference between the plateau borders and the three films associated with it which is shown in Fig.5.40 below. (Pugh 2005).

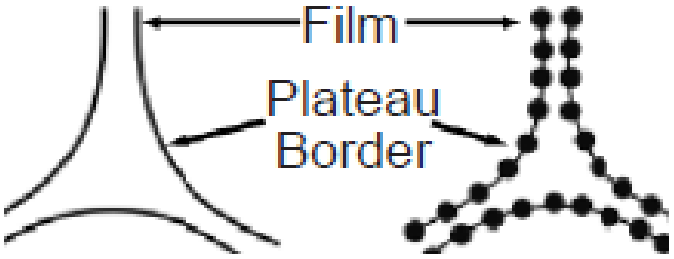

Fig. 5.40: The effect of particles on the pressure difference between the foam films and plateau borders (a) without particles (b) with particles

In the case of the foam with no particles as shown in Fig. 5.40 (a) the liquid in foam can flow from the film into the plateau border and then through the structure by gravity. Therefore when pressure drop is high, the flow rate is increased which causes faster drainage and the foam become less stable resulting less metal recovery. If many particles are attached to the gas/liquid interface as shown in Fig.5.40 (b) it will cause the pressure difference to decrease leading to a more stable froth.

In the second mechanism, the attached particles cause the overall drainage of foam to be hindered in the film and the liquid passages become constricted and tortuous. To some extent, the volume of the particles stabilized foam is therefore roughly proportionate to the amount of hydrophobic solids present between the foam film and the plateau borders.

The stability of the foam as an isolated system, free from thermal or mechanical perturbation, depends on its resistance to: (1) the gravitational drainage; (2) drainage by capillary suction, between regions with different radii of curvature and (3) gas diffusion through the liquid film induced by the pressure gradient between two bubbles. (Malysa 2008). Percentage recoveries of metal ions of cadmium, zinc, nickel, cadmium –PVP systems obtained under optimal pH conditions is shown in Table 5.4.

Table 5.4: Recovery of metals in large dia. column (metal concentration 100 ppm, metal :surfactant 1:2 molar ratio)

Metal	pH	Recovery (%)
Zn	8.25	5.63
Cd	2	2
Ni	8	1.12
Cd-PVP	8	1.072
Zn-Cd (Zn)	4	1.46
(Cd)	4	1.8
Ni-Cd(Ni)	10	0.4
(Cd)	10	6.26

The recovery of metals is considerably less which is largely influenced by the complex hydrodynamic pattern existing in such columns. There is large scale circulation, and bubbles group into clusters which are swirled upwards by turbulent eddies. Transient high speed channels are formed by chains of large bubbles. Outside these channels the bubbles move up slowly or are carried down by draining liquid results in dry foam .

Sublate formed traveled to top of column shown in Fig. 5.41(a). A naturally occurring internal foam fractionation takes place by the bursting bubbles. These bubbles coalesce frequently and burst almost immediately at the top of the foam brings sublate back to column resulting less percentage removal as shown in Fig. 5.41(b).

(a) **(b)**

Fig. 5.41: Foam column in operation for nickel removal (a) top of column and (b) intermediate height (Ni:SDS 1:2 molar ratio)

The lesson drawn from this exercise is that scale up of foam columns is not seamlessly continuous it can be at best piecewise continuous. Changing the scale of operation can result in absolutely distraught and unconnected results, one aspect that stands out is that hydrodynamics of the column has deep influence on the overall separation performances.

5.13 Conclusions:

The above experimental work shows that removal of heavy metals from feed solutions can be achieved by optimizing the levels of certain operating variables of foam separation techniques. This technique is useful for both analytical purpose as well as conventional industrial processes. The selection of a particular flotation technique depends on the concentration of metal present in the aqueous stream and the pH of the stream.

Heavy metals like cadmium, zinc and nickel recovery in the foamate, identification of the outlet for optimal recovery, effect of gas flow rate, pH, interaction of metal ions with a polymer on metal recovery, selective metal removal from binary systems of Zn-Cd and Ni-Cd were discussed in this chapter. Mechanism of metal recovery process, Effect of metal:SDS ratio, optimum pH for metals removal were identified using species distribution diagrams. For metal recovery as precipitated solids the particles formed were appropriately characterized. Floatation rate constants were evaluated and the separation was scaled to larger column size.